WATER FLOW AND TRANSPORT OF CHLORIDE IN UNSATURATED CONCRETE

A Thesis Submitted to the College of Graduate Studies and Research
in Partial Fulfillment of the Degree of Master of Science in
the Department of Civil and Geological Engineering,
University of Saskatchewan, Saskatoon, Canada

By
Ajeet Kumar

PERMISSION TO USE

In presenting this thesis in partial fulfillment of the requirements for a Postgraduate degree from the University of Saskatchewan, I agree that the Libraries of this University may make it freely available for inspection. I further agree that the permission for copying of this thesis in any manner, in whole or in part, for scholarly purposes may be granted by the professor or professors who supervised my thesis work or, in their absence, by the Head of the Department or the Dean of the College in which my thesis work was done. It is understood that any copying or publication or use of this thesis or parts thereof for financial gain shall not be allowed without my written permission. It is also understood that due recognition shall be given to me and the University of Saskatchewan in any scholarly use which may be made of any material in my thesis.

Requests for permission to copy or to make other use of material in this thesis in whole or in part should be addressed to:

Head of the Department of Civil and Geological Engineering,
University of Saskatchewan
57 Campus Drive
Saskatoon, Saskatchewan
Canada, S7N 5A9.

ABSTRACT

Concrete structures deteriorate in their operating environment under the combined action of harsh environmental conditions and external loading. Although the applied load can lead to a certain degradation of the structure, the main long-term deterioration mechanism involves moisture movement and the transport of chlorides within concrete. In order to build durable and reliable structures, it is necessary to be able to accurately predict the movement of moisture and chlorides within concrete.

In the case of unsaturated concrete, the transport of chloride ions is integrally associated with prediction of moisture fluxes in concrete. Even the diffusion of chloride ions depends on the degree of saturation of the concrete since concrete must have a continuous liquid phase for diffusion to occur. Therefore, simple diffusion theory, used in the current literature, is not sufficient to predict the diffusion of chloride ions in the case of unsaturated concrete. Most diffusion models described in the current published literature are applicable to concrete structures that are permanently wet and invariably underestimate the amount of chlorides penetrating the concrete of structures subjected to wetting and drying cycles. The research presented in this thesis reviews current knowledge, mathematical models and test methods pertinent to the movement of moisture and transport of chloride ions in unsaturated concrete.

A laboratory testing program was established to characterize the material properties of concrete mixes with water-cement ratios 0.4, 0.5 and 0.6. Concrete was characterized by its saturated hydraulic conductivity, moisture retention function and dependence of diffusion coefficient on degree of saturation. A geotechnical centrifuge was used to determine the saturated hydraulic conductivity of the concrete samples. Values of the saturated hydraulic conductivity of the samples were in the range of 10^{-11}-10^{-12} m/s.

The moisture retention function of concrete samples was determined using a vapour equilibrium technique. The experimental moisture retention data was used to determine van Genuchten parameters for each of the concrete mixtures and subsequently used to determine the capillary pressure-degree of saturation relationship and relative permeability-degree of saturation relationship as a ``closed- form`` analytical expression. An electrical resistivity technique was used to determine the dependence of the chloride diffusion coefficient on the degree of saturation of the concrete. The result was compared with the Millington and Quirk model. Most of the experimental results should be useful to researchers in the field, as well as the engineering community at large, considering that they are rarely found in the concrete literature.

Simulations were made to determine the influence of various parameters measured during experiment on movement of moisture and transport of chloride ions in unsaturated concrete using TOUGH2, a multiphase, multicomponent, model that simulates coupled heat, moisture and salt transport in saturated and unsaturated rocks.

ACKNOWLEDGEMENTS

This work would not have been possible without the whole-hearted support and encouragement of many individuals. Their contribution, in assorted ways to the research and the making of the thesis, deserved special mention. It is a pleasure to convey my gratitude to them all in my humble acknowledgment.

First and foremost, I want to thank the Department of Civil and Geological Engineering for giving me permission to commence this thesis in the first instance. I offer my sincerest gratitude to my supervisor, Dr. M. Boulfiza, who has supported me throughout my thesis with his patience and knowledge whilst allowing me the room to work in my own way. I am grateful to him for being a part of this project, which has proven to be very interesting and challenging at times.

I have to thank Professors S.L. Barbour, J. Sharma and B.F. Sparling, the members of my advisory committee, for their expertise, constructive criticism, guidance and valuable comments during the course of this research. Their involvement with originality has triggered and nourished my intellectual maturity that I will benefit from, for a long time to come.

I am grateful for the financial support provided by the Natural Sciences and Engineering Research Council of Canada (NSERC) and Intelligent Sensing for Innovative Structures (ISIS) Canada.

I would like to thank Mr. Alex Kozlow, Mr. Doug Fisher, Mr. Dale Pavier, for their assistance and direction throughout the laboratory component of the research.

My parents and family deserve special acknowledgement for encouraging me to pursue my degree. I have relied on their love and support throughout all my academics. Their unflinching courage and conviction always inspired me. It is to them that I dedicate this work.

I cannot end without thanking the friendly and cheerful group of fellow students, who helped and stood by me during the course of my stay at the University. I would also like to thank any others whom I may have missed, who have, directly or indirectly, contributed to my research.

Last but not the least; I would like to thank The Almighty, for having made everything possible by giving me strength and courage to do this work

Table of Contents

List of Figures

List of Tables

1 Introduction

1.1 Background

Service life prediction has emerged, over the last few years, as a major task in the design of concrete structures. The main long-term concrete deterioration mechanism involves moisture movement and the transport of dissolved harmful chemical species within concrete. In particular, the ingress of chlorides is a major cause of early deterioration of reinforced concrete structures. Although chloride ions in concrete do not directly cause severe damage to the concrete, they initiate and contribute to the corrosion of rebar in the structures when the chloride concentration at the surface of the rebar reaches a threshold level. The formation of rust is associated with large volume expansions which may result in cracking, spalling, and delamination of the concrete cover. In addition, severe corrosion reduces the load-carrying capacity of structures by reducing the cross-sectional area of reinforcement. In cold countries, the use of de-icing salt on roads and bridges in winter causes a premature deterioration of structures. Typically, bridge decks are exposed to cyclic wetting and drying conditions, and are subject to direct impact and repeated loading by traffic. These conditions, combined with salt applications, create a severe environment for the concrete.

One of the worst types of environmental exposure conditions leading to the premature degradation of structures is the case of concrete that is subject to repeated drying and wetting cycles. Although a very large number of concrete structures do operate under unsaturated conditions, most researchers in the concrete community have devoted their efforts to study transport of chloride in concrete under saturated conditions with little published data on the case of unsaturated concrete. Most diffusion models in the published literature are applicable to concrete structures that remain fully saturated at all times. They underestimate the amount of chloride penetrating a structure subjected to

wetting and drying cycles, as is the case for the splash and tidal zones of structures exposed to marine environments or for highway structures exposed to de-icing salts. Chloride profiles in these structures depend strongly on moisture fluctuation in the concrete cover. Other fields, such as soil physics and rock mechanics have made considerable progress in the modelling of unsaturated moisture movement by developing and/or applying the general theory of porous media which gives a powerful and consistent framework for addressing these issues.

1.2 Unsaturated Flow and Transport of Chlorides

In general, the pore space of concrete is not fully saturated (Kelham 1988; Hall 1989; Hall 1994). When the moisture content inside concrete is less than the saturation moisture content, water may be absorbed by the concrete through large capillary forces arising from the contact of the very small pores of the concrete with the liquid phase. This is an important mechanism of fluid invasion in concrete in most practical situations. Under unsaturated conditions, the water flux and subsequently the transport of dissolved chloride ions in response to a specified potential gradient is strongly dependent on the saturation of the material. The equilibrium state of water in an unsaturated porous material is characterized by its capillary pressure-degree of saturation function (also known as moisture retention function). Therefore, determination of the moisture retention function is necessary for the modelling of moisture flow and transport of chlorides in concrete. There has been very little effort to establish relationships for the capillary pressure as a function of degree of saturation for concrete.

Chloride diffusion can only occur if a continuous water phase is present in the capillary pores of concrete to provide a path for diffusion. Therefore, in the case of unsaturated concrete the diffusion process is hindered since the number of water filled pores decreases and that decreases the continuity of pore solution (Saetta et al. 1993). Under unsaturated conditions, the effective diffusion coefficient is no longer a constant but a function of saturation (Bazant and Najjar 1972; Garboczi 1990; Saetta et al. 1993; McCarter, et al. 2001) and therefore can not be described by simple diffusion theories that are typically used in the present literature. Dependence of the diffusion coefficient

on the degree of saturation is essential for determining the moisture flow and transport of chlorides in unsaturated concrete, in addition to the basic physical properties of concrete e.g. porosity, density, saturated hydraulic conductivity and moisture retention function. Up to now, relatively few authors, have focused on the effect of water saturation upon the diffusion coefficient in unsaturated porous materials, despite the fact that this is an essential component needed to model the transport of ions under unsaturated conditions. There is no direct experimental method found in the concrete literature to determine the dependence of the diffusion coefficient on the degree of saturation of concrete.

The complexity of the microstructure of concrete makes the theoretical and experimental investigation of its transport properties a great challenge. Depending on the mix design, preparation and environmental exposure, the material properties can be highly variable. The movement of moisture and the transport of chloride ions depend on a large number of factors such as porosity, pore size distribution, connectivity, and tortuosity. Currently, there are no standards test methods to measure key transport properties of concrete such as permeability and capillary- driven moisture transfer. However, some test methods developed and used by some other disciplines like soil sciences, rock sciences and petroleum sciences can also be used for concrete.

Multiphase multicomponent models are widely used for the determination of flow and transport processes in a porous medium. Concrete can be considered as a multiphase porous system where the pores are partly filled with liquid water and partly with a gaseous mixture of air and water vapour. In recent years, several models for simulating multiphase flow in porous media under unsaturated condition have been developed and can be very well used for concrete. These mathematical models normally consist of conservation equations (mass conservation of water, mass conservation of air, mass conservation of chlorides and energy conservation of the whole medium) completed by an appropriate set of constitutive equations (Darcy’s law of mass flux, Fick’s law of diffusion, capillary pressure, absolute and relative permeability, effective diffusion coefficient, effective thermal conductivity, etc.) as well as some thermodynamic

relationships. The decisive parameters which influence the flow and transport process can be determined experimentally.

1.3 Objective and Scope of Research

The overall objective for this research is to evaluate moisture flow and the transport of chlorides in unsaturated concrete. This objective is important for the evaluation of service life performance of concrete structures operating under unsaturated conditions. This will help in determining design criteria, which may enhance the service life performance of concrete structures.

The overall objective has been pursued through a series of more specific objectives. These specific objectives include: (1) developing a sound theoretical framework for evaluating moisture flow by using the developments from different fields other than concrete, such as soil science and the petroleum industry and apply them to the case of concrete; (2) experimental determination of the key parameters required for modelling moisture flow and transport of chlorides in unsaturated concrete, such as saturated hydraulic conductivity, moisture retention function and the dependence of the diffusion coefficient on the degree of saturation of concrete; and, (3) simulating moisture flow and transport of chlorides in unsaturated concrete using experimental parameters and determining the influence of those parameters on the movement of moisture and transport of chloride ions in unsaturated concrete.

The scope of the research work is limited to uncracked concrete. Chloride binding is also not considered while determining the transport of chlorides in concrete.

1.4 Research Methodology

The research methodology is divided into two components:

1. Laboratory Tests
2. Numerical Modelling

Laboratory tests involved the preparation of three standard concrete mixtures and the determination of key parameters such as the hydraulic conductivity, the moisture retention function and the diffusion coefficient-degree of saturation relationship, needed for modelling moisture flow and transport of chlorides.

The numerical modelling component involved using a multiphase multicomponent model simulator, TOUGH2, to evaluate the influence of various parameters measured during the experiments on the movement of moisture and transport of chloride ions in unsaturated concrete.

1.5 Outline of the thesis

Chapter 2 presents a review of current knowledge, mathematical models and test methods pertaining to the moisture flow and transport of chlorides in unsaturated concrete. The chapter focuses on identifying a sound theoretical framework for evaluating moisture flow by using the developments from different fields other than concrete, such as soil sciences and the petroleum industry and applying them to the case of concrete.

Chapter 3 presents all the details concerning the materials and methods used to perform the experiment. All the experimental procedures are presented as well as the method used to obtain the necessary parameters needed to model unsaturated moisture flow and transport of chlorides in unsaturated concrete.

Chapter 4 presents experimental determination of the necessary parameters needed to model unsaturated moisture flow and transport of chlorides in unsaturated concrete. The results of the experimental testing are discussed in this Chapter, the conclusions that can be drawn from the results as well as influence of various parameters measured during the experiments on the movement of moisture and transport of chloride ions in unsaturated by using a multiphase multicomponent model.

The last chapter present a summary of the research, the conclusion that can be drawn from the results and recommendations for future work.

2 Literature Review

Moisture movement coupled with transport of chlorides in concrete is one of the main causes of deterioration of concrete structures. This chapter presents a review of current knowledge, mathematical models and test methods pertinent to the main transport properties of unsaturated concrete. The main properties and transport mechanisms affecting moisture movement and chloride ions transport include permeability, capillary absorption, and diffusion.

2.1 Moisture movement in concrete

Concrete is a porous material and when the pores inside concrete are filled with water it is referred to as a saturated concrete. When the pores are occupied by both water and gas it is called unsaturated concrete. The movement of moisture and associated transport of dissolved chlorides depend on the saturation level of concrete. The driving potential for moisture movement in both saturated and unsaturated concrete is a pressure gradient.

2.1.1 Water flow under saturated conditions

Water movement under saturated conditions can be described by the well-known Darcy's Law. Darcy's Law states that the volumetric flow rate in one dimension through a porous medium is proportional to the cross-sectional area and the hydraulic gradient. Darcy's Law can be expressed as:

$$Q = -K\,A\frac{dh}{dl} \qquad [2\text{-}1]$$

where:

Q = volumetric discharge [m^3s^{-1}],

K = hydraulic conductivity [$m\ s^{-1}$],

A = cross-sectional area [m^2],

h = hydraulic head [m] = $(P/ \rho_w g) + z$

p = fluid pressure [N m^{-2}],

ρ_w = fluid density [kg m^{-3}],

g = acceleration due to gravity [m s^{-2}]

z = elevation [m]

l = flow path length [m], and

dh/dl = hydraulic gradient [-].

Hydraulic conductivity, K, also known as coefficient of permeability, is a function of the properties of the fluid and the porous medium in which the fluid flows. A more rational concept of permeability which is independent of the fluid properties and depends only on the characteristics of the porous medium is intrinsic permeability. Hydraulic conductivity and intrinsic permeability are related by the following equation:

$$K = \frac{k \rho_w g}{\mu} \qquad [2\text{-}2]$$

where:

k = intrinsic permeability [m^2], and

μ = dynamic viscosity of fluid [kg m^{-1} s^{-1}].

Equation [2-1] can be rewritten in terms of the Darcy flux or volume flux (q), defined as the flow per unit cross sectional area of the medium:

$$q = \frac{Q}{A} = - K \frac{dh}{dl} \qquad [2\text{-}3]$$

Although the volume flux has the units of velocity, it does not describe the velocity of fluid is flowing through the pores. This is due to the fact that only the portion of the medium that is filled with the fluid contributes to flow.

The law of mass conservation applies to any mass transport process and provides a differential equation which, when solved, gives the hydraulic head and flow rate in the flow domain. The continuity equation states that divergence ($\nabla \cdot$) of the mass flux

equals change in mass in a control volume. Under steady state, considering water to be incompressible (ρ_w is constant), the continuity equation can be written as

$$\nabla \cdot q = 0 \qquad [2\text{-}4]$$

2.1.2 Water flow under unsaturated conditions

In general, the pore space of concrete is not fully saturated (Kelham 1988; Hall 1989; Hall 1994). The degree of saturation of the pore space can depend on different factors such as relative humidity and the previous exposure of concrete to moisture. When the moisture content inside a concrete material is less than its saturation level, water may be absorbed into the concrete by large capillary forces arising from the contact of the very small pores of concrete with the liquid phase. This is an important mechanism of water flow into concrete that is often observed in field applications subjected to wetting/drying cycles.

Single phase flow

Richards (1931) was among the first authors to study the mechanism of water flow in unsaturated porous materials. The movement of water through the unsaturated zone is commonly described using Richards' equation. Darcy's Law, which has been applied to saturated flow in porous media, can be generalized to unsaturated water flow where it can be written for the liquid phase as (Scheidegger 1974):

$$q_l = -\frac{k \,.\, k_{rl}}{\mu_l}(\nabla P_l - \rho_l g) \qquad [2\text{-}5]$$

where q_l is the volumetric flux of the liquid phase, k is the intrinsic permeability, k_{rl} is the relative permeability of liquid, ρ_l is the liquid phase density and P_l is the liquid phase pressure.

Richards applied a continuity requirement to Darcy's law, and obtained a general partial differential equation describing water movement in unsaturated soils. He proposed the following equation to describe the flow of water under capillary suction:

$$\frac{\partial(\phi S_l)}{\partial t} = -\nabla \cdot q_l \qquad [2\text{-}6]$$

where ϕ is the porosity and S_l is the saturation of the liquid phase.

This equation assumes that the water - air system can be simplified by considering air to be infinitely mobile and neglecting the effect of displaced air during liquid flow. The pressure in the air phase is then zero gauge everywhere and spatial derivatives of the air phase pressure are zero as well. As a result, only the wetting phase equation is necessary to describe the flow system. Combining equations [2-5] and [2-6] results in the wetting phase equation referred to as Richards' equation:

$$\frac{\partial(\phi S_l)}{\partial t} = -\nabla \cdot \left[\frac{k.k_{rl}}{\mu_l} (\nabla P_l - \rho_l g) \right] \qquad [2\text{-}7]$$

Multiphase multicomponent models

Multiphase multicomponent models are more general models widely used for the determination of flow in porous media in situations where Richards' equation is no longer adequate. Multiphase multicomponent models are a generalisation of the modelling used in two-phase flow to cases where more than two phases are present. The 'phase state' indicates which phases are present locally in the control volume. Darcy's Law, which has been applied to single phase flow in porous media, can be generalized for multiphase flow or unsaturated flow assuming that the flow of a phase in the presence of another phase can be viewed as a single phase flow through a reduced pore network, with permeability replaced by phase permeability, and is written for phase α as (Scheidegger 1974):

$$q_\alpha = -\frac{k.k_{r\alpha}}{\mu_\alpha} (\nabla P_\alpha - \rho_\alpha g) \qquad [2\text{-}8]$$

where q_α is the volumetric flux in the fluid phase (liquid or gas) α, $k_{r\alpha}$ is the relative permeability, and P_α is the fluid pressure in phase α. Relative permeability quantifies the interference of one phase with the other and varies between 0 to 1. Each of the phases is considered to have a separately defined volume fraction with the sum equal to unity. The

pressure P_α in phase α is the sum of the pressure P of a reference phase (usually taken to be the gas phase), and the capillary pressure $P_{c\alpha}$.

$$P_\alpha = P + P_{c\alpha} \quad [2\text{-}9]$$

In general, capillary pressure is defined as the pressure difference between the non-wetting phase (air) and the wetting phase (water) (Bear 1972). Capillary pressure depends on the saturation of concrete and is expressed as:

$$P_g - P_l = P_c(S_l) \quad [2\text{-}10]$$

The movement of each phase through an unsaturated porous media occurs under the combined action of gravity, and pressure forces and can be described by the general mass balance equation as (Scheidegger 1974; Dullien 1992):

$$\frac{\partial(\phi \rho_\alpha S_\alpha)}{\partial t} + \nabla \cdot (\rho_\alpha q_\alpha) = F_\alpha \quad [2\text{-}11]$$

where ϕ is the porosity, ρ is the density of phase α, S is the saturation of phase α , or fraction of void space occupied by phase α, F is a source or sink term, and $\nabla \cdot (\rho_\alpha q_\alpha)$ is the divergence of fluid flux. Mass balance equation for each phase can be written separately.

Using the multiphase multicomponent mathematical models one could consider concrete as a multiphase multicomponent porous material. The pore volume of concrete is considered to be occupied by two phases: water (index *l*) and gas (index *g*). The phases are considered to be immiscible (i.e. separate from each other). The two fluid components of interest in the case of concrete are water and air; each of which can partition into each phase. The gas phase is treated as a mixture of air and water vapour, where each constituent may exist in any fraction between zero and one. On the other hand, the liquid phase is mostly water, although small amounts of dissolved air can exist in solution. For the non-isothermal multiphase processes taking place in the porous media under consideration, the assumption of local equilibrium is valid since flow velocities are small. Effects of hysteresis in the constitutive relationships are not accounted for. Component mass balances are developed under the assumption of

thermodynamic phase equilibrium. Component balance equations for water and air take the form:

$$\left\| \begin{array}{l} \frac{\partial d_w}{\partial t} + \nabla \cdot M_{\mathbf{w}} = F_{\mathbf{w}} \\ \frac{\partial d_a}{\partial t} + \nabla \cdot M_{\mathbf{a}} = F_{\mathbf{a}} \end{array} \right. \qquad [2\text{-}12]$$

where d_w (d_a) is the bulk density of water (air), $M_{\mathbf{w}}$ ($M_{\mathbf{a}}$) denotes the net mass flux of water (air), and $F_{\mathbf{w}}$ ($F_{\mathbf{a}}$) denotes mass source for water (air). The bulk density is given by:

$$\left\| \begin{array}{l} d_w = \phi \left(X_{wl}\, \rho_l\, S_l + X_{wg}\, \rho_g\, S_g \right) \\ d_a = \phi \left(X_{al}\, \rho_l\, S_l + X_{ag}\, \rho_g\, S_g \right) \end{array} \right. \qquad [2\text{-}13]$$

where X_{wl} (X_{al}) denotes the mass fraction of the water (air) component in the liquid phase, X_{wg} (X_{ag}) mass fraction of the water (air) component in gas phase, ρ_l (ρ_g) is the liquid (gas) phase density, S_l (S_g) is the liquid (gas) phase saturation, and ϕ is the porosity. The pore space is assumed to be fully occupied by the fluid phase, and hence, $S_l + S_g = 1$.

The water and air net mass fluxes appearing in the balance equation [2-12], are assumed to be a superposition of component fluxes in each phase,

$$M_w = M_{wl} + M_{wg} \qquad [2\text{-}14]$$

where $M_{\mathbf{w}l}$ denotes the net mass flux of water in the liquid phase, and $M_{\mathbf{w}g}$ denotes the net mass flux of water in the gas phase. Mass flux of dissolved air in the liquid phase has been neglected. Each component phase-flux can be written as a sum of an advective flux and a diffusive flux,

$$\left\| \begin{array}{l} \left\{ \begin{array}{l} M_{wl} = X_{wl}\, \rho_l\, q_l + \mathrm{J}_{wl} \\ M_{wg} = X_{wg}\, \rho_g\, q_g + \mathrm{J}_{wg} \end{array} \right. \\ M_a = X_{ag}\, \rho_g\, q_g + \mathrm{J}_{ag} \end{array} \right. \qquad [2\text{-}15]$$

where $J_{\kappa\alpha}$ is the diffusive flux of component κ in the bulk of fluid phase α. The advective fluxes are assumed to be properly described by the extended Darcy law, in which relative permeabilities are introduced to account for the multiphase motion of fluids as defined by equation [2-8]. Assuming that each phase has its own phase pressure, the mass fluxes of liquid and gas phases are given by

$$\left\| \begin{array}{l} q_l = -\dfrac{k_{rl}}{\mu_l} k \cdot \left(\nabla P_l - \rho_l \, \mathrm{g} \right) \\ q_g = -\dfrac{k_{rg}}{\mu_g} k \cdot \left(\nabla P_g - \rho_g \, \mathrm{g} \right) \end{array} \right. \qquad [2\text{-}16]$$

where $P_l(P_g)$ is the liquid (gas) phase pressure. The phase pressures are related via the capillary pressure as defined by equation [2-9].

It is clear from equation [2-16], both the capillary pressure-saturation function and relative permeability-saturation function are fundamental for a realistic modelling of moisture flow in unsaturated concrete. The common parameter, degree of saturation, serves to link the two constitutive relationships and provides further coupling of the flow equations through the additional constraint that the fluid saturations must sum to unity.
The equilibrium state of water in an unsaturated porous material is characterized by its capillary pressure-saturation function, $P_c(S_l)$, also known as moisture retention function. The Van Genuchten mathematical model (1980) which is based on Mualem's research (1976), has been used extensively for representing the moisture retention function in the field of soil sciences and has been validated for concrete by Savage (1997) and used by others (Mainguy et al. 2001; Monlouis et al. 2004; Pont et al. 2004). While it remains a challenge to measure relative permeability in concrete, it is reasonable to expect that some of the experimental methods developed in the field of soil sciences to determine relative permeability should be applicable to concrete (Hall 1989; Dullien 1992).

One alternative to the direct measurement of the relative permeability is to use theoretical methods which predict the permeability from more easily measured moisture retention data. Measured moisture retention data can be expressed by means of closed-form analytical expressions which contain parameters that are fitted to the observed data.

The use of analytical functions allow for a more efficient representation of the hydraulic properties and at the same time provide a method for interpolating or extrapolating to parts of the retention or permeability curves for which no data are available.

Relative permeability and the capillary pressure are represented by the van Genuchten-Mualem model (Mualem 1976; van Genuchten 1980) and van Genuchten function (1980), respectively.

$$k_{rl} = \sqrt{S^*}\{1-(1-[S^*]^{1/m})^m\}^2 \qquad [2\text{-}17]$$

$$P_c = -\frac{1}{\alpha}\left((S^*)^{-\frac{1}{m}}-1\right)^{\frac{1}{n}} \qquad [2\text{-}18]$$

$$S^* = \frac{(S_l - S_{lr})}{(1-S_{lr})} \qquad [2\text{-}19]$$

where m, n and α are empirical material parameters , with m=1-1/n

The diffusive fluxes of component κ in phase α are given by

$$J_{\kappa\alpha} = -\phi\tau_0\tau_\alpha\rho_\alpha D_{\kappa\alpha}\nabla X_{\kappa\alpha} \qquad [2\text{-}20]$$

where ϕ is porosity, $\tau_0\tau_\alpha$ is the tortuosity of the porous medium, ρ_α is the phase density and, $D_{\kappa\alpha}$ is the diffusion coefficient of component κ in the bulk of fluid phase α.

Although chloride transport can be represented by the above equation, only diffusive fluxes of water and air will be described here. The transport of chlorides will be discussed in section 2.2. Application of equation [2-20] to the case of water and air yields the following equations.

$$\begin{Vmatrix} J_{wl} = -\phi\tau_0\tau_l\rho_l D_{wl}\nabla X_{wl} \\ J_{wg} = -\phi\tau_0\tau_g\rho_g D_{wg}\nabla X_{wg} \\ J_{ag} = -\phi\tau_0\tau_g\rho_g D_{ag}\nabla X_{ag} \end{Vmatrix} \qquad [2\text{-}21]$$

2.1.3 Experiments

In order to measure key transport properties of any materials, standard experimental test methods are needed. Without standard experimental test methods, it is difficult to develop criteria needed for the prediction and assessment of the service life of concrete structures. Currently, there are no standard test methods for measuring key transport properties of concrete, such as permeability and capillary- driven moisture transfer. The following sections explain experimental methods used to determine the major transport properties of porous materials. The methods discussed here are not only from the field of concrete, but also from soil sciences and the petroleum industry.

Determination of saturated permeability

Saturated permeability measurements are often made on small-scale laboratory samples. Although there are numerous Portland Cement Concrete (PCC) permeability measurement methods, none is recognized as a standard test method. In one method, borrowed from soil science, a head of water is placed above the concrete sample and then the height of the head is monitored over time to determine the volumetric flow through the concrete. The permeability of the sample is then determined using Darcy's law. The main drawback of this method is that it may take weeks or longer to obtain sufficient flow to determine permeability due to the low permeability of concrete. For low hydraulic gradients and reasonable sample sizes, the quantity of flow through a sample can be expected to be quite small. The value of saturated permeability for typical concrete is 10^{-12} m^2. These values of permeability are orders of magnitude lower than for common porous media such as soil and sandstone rock and, hence, are much more difficult to measure.

To establish even a small flow rate through concrete requires a relatively high pressure and an effective seal is required during the test to reduce leakage of fluids along the side [Martys 1995]. Therefore, most permeability tests require the application of high pressures and the use of custom made permeameters for measurement of the permeability of concrete. The test method is difficult to standardize due to different test

pressures, duration of the test, methods used to seal the specimen in the cell, and test procedures (Nyame and Illston 1981; Nyame 1985; Dhir et al. 1989; Ludirdja et al. 1989; El-Dieb and Hooten 1994).

The most direct experimental arrangement for determining permeability involves measuring the steady flow of water through a sample of uniform cross- sectional area with the sample sides sealed to prevent leakage and the flow under an applied pressure (Basheer 2001). For a constant head setup, the coefficient of permeability is calculated from the knowledge of sample geometry and fluid characteristics, together with the measurement of flow rate and applied pressure using equations [2-1] and [2-2]. For a falling head setup, the flow rate is measured under the action of diminishing pressure head. If during the test, the level of water in the water tube falls from an initial height h_0 at $t=0$ to some height h_t at time t, the permeability of the concrete sample is calculated as follows:

$$K = \frac{aL}{At} ln \frac{h_0}{h_t} \qquad [2\text{-}22]$$

where a = cross-sectional area of water tube

A = cross sectional area of the sample, and

L = length of the specimen parallel to the direction of flow.

In addition to the traditional permeability cell which is commonly used to measure the permeability of a concrete, there are some other methods which also can be used for determining the permeability of concrete. A geotechnical centrifuge is one of them. Geotechnical centrifuges have been used in recent years to understand and simulate transport mechanisms in soils under accelerated–gravity environments. The centrifuge can be used in two very distinct ways: as a testing apparatus to obtain characteristic parameters, such as hydraulic conductivity and diffusion coefficient; and as a modelling apparatus to examine theory and in order to validate the capabilities of numerical simulations (Alemi et al. 1976; Cargill and Ko Hon-Yim 1983; Arulanandan 1988; Mitchell 1991; Mitchell 1994; Singh and Gupta 2000; Khanzode et al. 2002; Singh and Kuriyan 2002). When used for testing, no real prototype is actually modelled in the

centrifuge and the capabilities of the machine are utilized to produce data from which parameters can be derived.

The principles of both standard permeability cell technique and centrifuge technique are described in the following sections.

a) Permeability Cell Technique

The most commonly used test set-up (Figure 2-1) consists of a permeability cell to hold the sample, a set of inlet controls to admit water at the specified pressure while measuring the inflow, and a set of outlet controls to allow the discharge from the test specimen to be monitored along with the outlet pressure. The permeability cell itself is specifically made to seal the sides of the specimen and allow the permeating liquid, usually water, to go through the sample without any leakage. The coefficient of permeability is then calculated from the sample geometry, fluid characteristics, flow rate and applied pressure using Darcy's law.

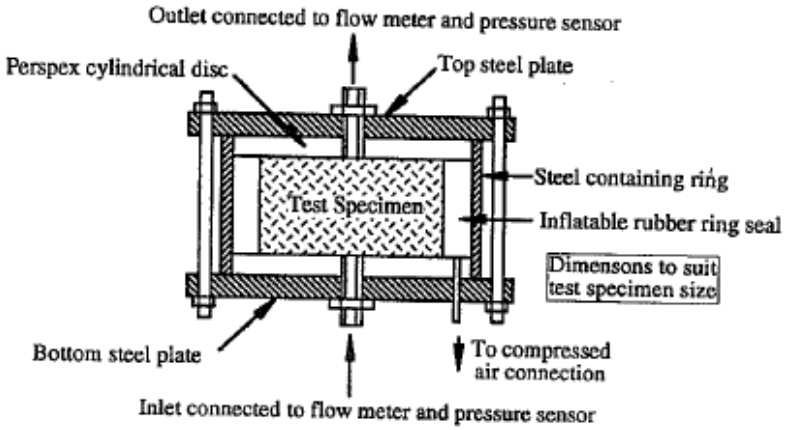

Figure 2-1: A typical permeability cell

b) Centrifuge Technique

The magnitude of the acceleration experienced by the sample in a centrifuge with an operative centrifuge radius of R, and a rotational speed of ω is given by:

$$a_{cen} = \omega^2 R \qquad [2\text{-}23]$$

The increase in the sample acceleration is used to define the centrifuge scale factor *N:*

$$N = \frac{a_{cen}}{g} \qquad [2\text{-}24]$$

For centrifuge studies involving flow of fluids, it has been established (Goodings 1985; Mitchell 1991) that an *N*-fold increase in gravity in a centrifuge model results in an *N*-fold increase in velocity of flow through soil over that in the prototype.

When introducing the scale factor, the falling head setup equation [2-22] changes to

$$K = \frac{1}{N}\frac{aL}{At} ln \frac{h_0}{h_t} \qquad [2\text{-}25]$$

When analyzing the above two experimental methods it was realized that the centrifuge technique was the more suitable method for determining the permeability of concrete considering the short duration of the tests. The permeability of concrete can be measured within a day using a centrifuge.

Unsaturated Water Movement

Under unsaturated conditions, the water flux occurring through a porous material in response to a specified potential gradient is strongly dependent on the saturation of that material. As discussed earlier, capillary pressure-saturation relationships and relative permeability-saturation curves describe this dependence. Direct measurement of relative permeability in concrete is still a challenge and a subject of considerable research. Typically, these relationships are estimated using water retention and saturated hydraulic conductivity measurements and fitting them to a particular mathematical model (e.g., Mualem 1976; van Genuchten 1980). Within numerical models, these relationships can be represented by specific mathematical functions containing one or more fitted parameters. The parameters are fitted to the moisture retention data. Therefore, water retention data needs to be determined first to get those parameters.

The equilibrium water saturation inside concrete at a given capillary pressure, P_c, depends on the process corresponding to either material drainage or imbibition i.e. water retention in concrete exhibits hysteresis. Models have been developed for describing this hysteresis (Lenhard and Parker 1987; Parker and Lenhard 1987; Meyer et al. 2004), but the data on which the parameters of hysteresis can be estimated are often not available.

There are two common methods found in the literature for measuring the moisture retention relationship for a porous material using controlled-suction techniques. The experimental methods are described in the following sections:

a) Pressure Membrane Technique

The pressure membrane technique was developed based on the fundamental definition of matric suction. Matric suction, *Pc*, is defined as the pressure difference across the air-water interface, namely (P_a-P_w), where P_a is the pore air pressure and P_w is the pore water pressure. In a pressure plate extractor, the pore water pressure is maintained as a constant, usually at zero pressure, while the air pressure is elevated to produce the desired matric suction (Richards 1941, ASTM D3152-72 1977; ASTM D2325-68 1981). A porous ceramic disk is used that allows air and water pressure to be applied separately. The ceramic disk is a high air entry disk that allows water to readily flow through the ceramic disk, while restricting airflow up to certain pressure. The air pressure required to cause air to flow through the disk is called the air entry pressure of the high air entry disk being used.

In the case of a draining sample, the experiment is started with an initially saturated sample. The saturated sample is sealed inside the pressure vessel and the internal gas pressure is raised to a predetermined level. The sample is allowed to equilibrate at the new pressure. Once the sample is at equilibrum, the pressure vessel is opened and the sample is taken out and weighed to determine its gravimetric water content. It may take days or weeks for the sample to attain equilibrium water content at any predetermined value of pressure. The sample is subjected to multiple predetermined pressures and the

water content is measured at each step. The wetting data are obtained starting at a high pressure with an initially dry sample.

The pressure membrane technique is used frequently in soil sciences. However, this technique can only be used for suction up to 14 MPa (Tang and Cui 2005). The capillary pressure value of concrete over the full range of saturation is very large in comparison to that of soil. A sufficiently large gas pressure is needed to overcome the suction forces in the low saturation range for concrete (Hall and Hoff 2002). Therefore, the pressure membrane technique can be only used for high saturation levels of concrete, and hence, is not commonly used for concrete.

b) Vapour Equilibrium Technique

The vapour equilibrium technique is widely used for measuring moisture retention data of concrete (Savage and Janssen 1997; Baroghel-Bouney et al. 1999; Romero et al. 2001; Homand et al. 2004; Tang and Cui 2005) since the pressure required to remove water from concrete is much greater than that which could be obtained by most other techniques (Hall 1989; Hall 1994; Martys 1995). This technique can be used for suctions ranging from 3 to 1000 MPa (Romero et al. 2001; Tang and Cui 2005). The capillary pressure of water in a porous material can be determined from measurements of the vapour phase in equilibrium with the liquid phase in the pores (Rockhold et al. 1993). When a porous material is placed in an environment of controlled humidity, it either takes or releases water until its vapour pressure becomes equal to that of its environment. The water content of the material at equilibrium can then be determined by weighing the sample. For a given temperature T, the vapour pressure and the total suction, summation of capillary pressure and osmotic pressure, are connected through Kelvin's equation:

$$P_c = -\left(\frac{RT}{M}\right)\ln\left(\frac{p}{p_s}\right) \qquad [2\text{-}26]$$

where,

P_c= total suction (MPa)

M= molecular weight of water vapour (0.01802 kg mol^{-1})

R= ideal gas constant (8.3143×10^{-3} kg MPa mol^{-1} K^{-1})

T = Temperature of the liquid phase in Kelvin (° C + 273.16)

p = water vapour pressure in equilibrium with the liquid phase (Pa)

p_s= saturated water vapour pressure at temperature T(Pa)

If the osmotic pressure is negligible, the total suction is equivalent to the capillary pressure (matric suction) defined in the equation [2-26]. Bailey and Hampsen (1982) estimated that the osmotic pressure for cement is approximately ≈ 0.03MPa. This value of osmotic pressure is considered to be very small in comparison to the capillary pressure of concrete. Therefore the total suction in the equation [2-26] can safely be considered to be equal to the capillary pressure, without any corrections for osmotic pressure (Rockhold et al. 1993; Savage and Janssen 1997; Baroghel-Bouney et al. 1999) while calculating water retention parameters.

Saturated salt solutions are normally used in the vapour equilibrium technique. The advantage of using a saturated solution is that the molar fraction of water in solution does not change as water vapour exchanges between the liquid phase and the gaseous phase. The imposed suction, which is related to the molar fraction of water, is therefore kept constant (Tang and Cui 2005).

The experiment consists of putting samples of concrete into relative humidity (RH) controlled sealed cells, and subjecting the samples to a step-by-step desorption. Each step lasts until moisture equilibrium is reached inside the sample. Each relative humidity atmosphere represents a different constant boundary condition. The capillary pressure corresponding to the relative humidity boundary condition is calculated using Kelvin's equation [2-26]. The attainment of equilibrium is assured by checking the mass constancy of the samples. Once the sample attains a constant weight over time and there is no further decrease in the weight of the sample, the corresponding equilibrium weight of the sample is measured with their natural water contents, m_h, just after removing them from their controlled humidity enclosures. The sample is then oven dried at 105 °C for 24 hours to measure the dry weight, m_d. The degree of water saturation for the sample is then determined by using:

$$S_l = \frac{m_h - m_d}{m_s - m_d} \times 100 \qquad [2\text{-}27]$$

This method is well established and most commonly used for determining moisture retention curves or water vapour desorption isotherms (meaning “equilibrium mass water content vs. RH curves) of concrete. In order to obtain such curves, water vapour sorption experiments are normally carried out at a temperature of 22 ± 1°C on thin samples. For concrete usually the typical size of the sample is ~20 mm in diameter and ~2 mm in thickness (Hall and Hoff 2002).

2.2 Chloride Transport

Capillary sorption, diffusion and permeation are the three major processes by which chloride ions can penetrate concrete. In the case of saturated concrete, chloride ions penetrate concrete under a chloride ions concentration gradient known as diffusion. Concrete must have a continuous liquid phase for diffusion to occur. Diffusion is usually the dominant transport mechanism for chloride ions ingress in the case of fully saturated concrete.

A more common transport mechanism in other porous media and unsaturated concrete is advection through capillary sorption. When water (possibly containing chlorides) encounters a dry surface, it is drawn into the pore structure though capillary suction. Advection through capillary suction is the dominant transport mechanism for chloride ions in the case of unsaturated concrete.

Another mechanism for chloride ingress is advection through permeation, driven by moving fluids under pressure gradients. If there is an applied hydraulic head on one face of the concrete and chlorides are present, they may permeate into the concrete. A situation where a hydraulic head is maintained is rare for most practical situations, however.

2.2.1 Chloride transport by diffusion

Chloride diffusion results in chloride transport from regions of high chloride ions concentration to regions of lower ions concentration and occurs as a result of the random motion of molecules and atoms. Chloride ions move through the pore solution of concrete due to concentration gradient within the pore solution. Under steady state conditions, the diffusion of ions in a porous medium is usually described by Fick's 1^{st} law of diffusion, according to which the rate of transfer of diffusing chlorides through a plane perpendicular to the direction of diffusion is proportional to the gradient of the concentration of free chloride ions, which for one-dimensional flow, is given by:

$$J = -D_{eff} \frac{\partial C}{\partial x} \qquad [2\text{-}28]$$

where J is the flux of chlorides due to diffusion in the x-direction (kg/m^2.s), D_{eff} is the effective chloride diffusion coefficient of concrete (m^2/s), and C is the concentration of chlorides dissolved in the pore solution (kg/m^3 of pore solution) at depth x. The negative sign in equation [2-28] indicates that diffusion occurs in the opposite direction to that of increasing concentration. In practical terms, equation [2-28] is only useful after the steady-state condition has been reached, i.e. there is no change in concentration with time.

When the concentration of chloride ions inside concrete changes with time (i.e., transient condition) the law of mass conservation in an infinitesimal volume of the pore solution of concrete gives the changes with time of the chloride ions concentration in that unit volume of concrete, often referred to as Fick's Second Law:

$$\frac{\partial(\phi S_l C)}{\partial t} = -\frac{\partial J}{\partial x} \qquad [2\text{-}29]$$

The term on the left hand side represents the rate at which chloride ions enter inside the concrete and the term on the right hand side represents divergence of chloride flux in pure solution. In a porous medium, the cross-sectional area available for diffusion in the aqueous phase is reduced by the volume fraction of the void space present inside the porous medium, known as porosity. The above equation changes to:

$$\frac{\partial(\phi S_l C)}{\partial t} = \frac{\partial}{\partial x}(D_{eff}\frac{\partial C}{\partial x}) \qquad [2\text{-}30]$$

where ϕ is the porosity.

A closed-form solution of equation [2-30] for the initial condition C(x >0, t=0) = 0 (the initial concentration in the concrete is 0) and boundary condition C(x =0, t >0) = C_0 (the surface concentration is constant at C_0) for a semi-infinite medium, can be shown to be as follows (Crank 1975):

$$\frac{C(x,t)}{C_0} = 1 - erf(\frac{x}{\sqrt{4D_{eff}t}}) \qquad [2\text{-}31]$$

where $C(x,t)$ is the concentration of chlorides at depth x after time t (kg/m^3 of pore solution), C_0 is the chloride concentration at the surface (kg/m^3 of solution) and *erf* is the error function. This solution is only valid when both the diffusion coefficient and the surface concentration are assumed to be constant in space and time.

Chloride diffusion is a process which can only occur if water is present in the capillary pores of concrete and provide a continuous path for diffusion. Therefore, in the case of unsaturated concrete, the diffusion process is hindered since the number of water filled pores decreases and that decreases the continuity of pore solution (Saetta et al. 1993). Under unsaturated conditions, the effective diffusion coefficient is no longer a constant but is a function of saturation as defined below:

$$D_{eff} = D_o\phi\beta \qquad [2\text{-}32]$$

where D_o is the diffusion coefficient in a continuum, e.g., ionic diffusion coefficient in bulk water, ϕ is the porosity and β is a pore structure parameter, discussed below.

The diffusion paths in a porous medium are usually constrained by pore structures that are tortuous, non-uniform in cross-section and constricted or disconnected at certain points (Atkinson et al., 1984). These considerations of diffusion in the porous medium are reflected by the parameter β. If all the pores were straight, non intersecting tubes, the factor β would be one. Its value, however, will always be less than one, and takes into

account all the tortuosity and connectivity of the pore network (Garboczi 1990). It is a function of the pore structure and degree of saturation (S_l) of the pores (Bachmat et al. 1986; McCarter et al. 2001):

$$\beta = \tau_o \, \tau_\beta \qquad [2\text{-}33]$$

where, τ_o is a porous medium dependent factor and τ_β depends on phase saturation. The saturation dependence on tortuosity is not well understood at present in the field of concrete. No method could be found in the literature to evaluate β directly under unsaturated conditions.

The Millington and Quirk (1961) model for variably saturated porous media, has frequently been used in concrete (Mainguy et al. 2001; Pont and Ehrlacher 2004). The tortuosity factor in Millington and Quirk model is expressed as:

$$\beta = \phi^{1/3} \, S_l^{10/3} \qquad [2\text{-}34]$$

where, ϕ is porosity and S_l degree of saturation of concrete.

2.2.2 Chloride transport by advection

Transport by advection is the transport of chloride ions associated with the movement of water in which they are dissolved. It is mathematically described as the product of the moisture flux through concrete and the concentration of dissolved chloride ions. The advective flux of chloride ions is given as:

$$\begin{cases} J'_{sat} = C \cdot q \\ J'_{unsat} = C . q_l \end{cases} \qquad [2\text{-}35]$$

where J'_{sat} is the advective flux of chloride ions (kg/m^2.s) in saturated case, J'_{unsat} is the advective flux of chloride ions (kg/m^2.s) in unsaturated case, q is the moisture flux given by equation [2-3] and q_l is the moisture flux given by equation [2-5].

A dimensionless number characterizing the relative strength of advection and diffusion is the Peclet number, P_e. When P_e is >> 1, advection dominates, and when P_e << 1, diffusion dominates (Martys 1995). In the majority of practical situations; involving

unsaturated transport through concrete, P_e>10 (Puyate and Lawrence, 1998). The high value of Peclet number suggests dominance of advective flow over diffusive flow in case of unsaturated transport through concrete.

2.2.3 Experiments

As discussed earlier, characterizing the dependence of the diffusion coefficient on the degree of water saturation is essential for an accurate determination of moisture flow and transport of chlorides in unsaturated concrete, in addition to the basic physical properties of concrete e.g. porosity, density, saturated hydraulic conductivity and moisture retention function. Up to now, relatively few authors have focused on the effect of degree of water saturation upon the diffusion coefficient in unsaturated porous materials, despite the fact that this is an essential component needed to model the transport of ions in multiphase flow simulators. No direct experimental method could be found in the concrete literature for determining the dependence of the diffusion coefficient on the degree of water saturation of concrete.

Direct and indirect techniques have been used to measure diffusion coefficients in porous media. Fick's first law is used for evaluating steady state experiments, while Fick's second law is used for transient state experiments. The diffusive fluxes through unsaturated porous materials of low porosity, e.g. gravel, concrete are anticipated to be many orders of magnitude lower than in pure solution. Due to its lower magnitude, very long time periods are needed to collect sufficient data from transient experiments. Moreover, it is very difficult to maintain proper boundary conditions; in addition, the experimental setup is not easy (Conca and Wright 1990). Therefore, indirect methods are used to measure diffusion coefficients in unsaturated porous materials of low porosity. The most widely used indirect method is the measurement of electrical conductivity or electrical resistivity, which provides reliable estimates of diffusion coefficients in unsaturated porous materials (Atkinson et al. 1984; Conca and Wright 1990).

The Resistivity technique is an indirect method that has been used reliably to estimate diffusion coefficients in unsaturated porous materials. The electrical resistivity of concrete shows a strong dependence on the degree of saturation and type of concrete. Furthermore, the electrical resistivity of a porous material is related to its effective diffusion coefficient (Atkinson et al. 1984; Garboczi 1990). Also, the experimental measurement of resistivity of unsaturated concrete can be used to get a relationship between the diffusion coefficient and the degree of saturation of concrete.

The "salt ponding test" is one direct experimental method which at least in part, depends on capillary transport, which has frequently been used in the concrete literature. Unfortunately, even the salt ponding test does not separate capillary effects from pure diffusion (Martys 1995; Martys and Ferraris 1997) and at the same time it is very difficult to characterize the result of this test. The experimental data from this test can not be used in models to predict the long term durability of concrete structure due to its qualitative nature and can only be used to compare different concrete qualities.

The principles of the two experimental methods are described in the following section:

a) AASHTO T259: Salt Ponding Test

The salt ponding test is a commonly used test for determining the ingress of chlorides into concrete which, at least in part, depends on capillary transport. Test samples of size 300x300x75 mm are immersed on the top surface with 3% (0.5 M) sodium chloride solution for a period of 90 days. Prior to the test, the samples are moist cured for 14 days, then stored in a drying room at 50 percent relative humidity for 28 days before applying the salt solution. The penetration of chloride ions is then monitored by taking cores and measuring the amount of acid-soluble chlorides as a function of depth.

Since the concrete samples are dried for four weeks prior to the ponding test, it is likely that capillary transport is the main driving mechanism for the chloride ion transport, at least during the early times. But, it is not clear how the ponding test separates capillary effects from pure diffusion (Martys 1995; Martys and Ferraris 1997). It is very difficult to characterize the result of this test since two different transport mechanisms may be

present in the structure at the same time and the relative importance of each is not necessarily reflected by this test procedure. The relative amount of chloride ions penetrated into the concrete by capillary absorption to the amount entering by diffusion will be greater when the test is only 90 days than when compared to the relative quantities entering during the lifetime of a structure (Stanish et al. 1997).

b) Resistivity Techniques

Resistivity techniques can be used indirectly to measure the dependence of the diffusion coefficient on the degree of water saturation of concrete. For cementitious materials, the diffusion process usually considered is that of the diffusion of ions through water-filled pores. The effective diffusion coefficient (D_{eff}) and the electrical conductivity (σ)of a porous material can be expressed by the following relationship with the pore structure parameter (Atkinson et al. 1984; Garboczi 1990):

$$\frac{D_{eff}}{D_o} = \frac{\sigma}{\sigma_o} = \phi\beta \qquad [2\text{-}36]$$

where D_o is the diffusion coefficient in a continuum, σ is the conductivity (Siemens/m) of the porous material, when it is regarded as an effective medium, σ_o is the conductivity in a continuum, e.g., conductivity in bulk water, ϕ is the porosity and β is a pore structure parameter.

For a concrete sample, if the conductivity of the pore fluid remains constant over time, the bulk conductivity of the concrete would be controlled by the level of pore saturation only. As the level of saturation in the capillary pores changes, there is a change in the bulk electric properties of concrete which can vary over several orders of magnitude. Saturated concrete ($S_l \approx 100$ %) behaves as an electrolyte with a typical resistivity of about 50 Ωm, which is within the range associated with semiconductors. However, dry concrete ($S_l \approx 0$ %) shows a resistivity of around 10^9 Ωm (Nilsson et al. 1996).

The conductivity of the material is defined as the reciprocal of resistivity, ρ, i.e.

$$\sigma = \frac{1}{\rho} \qquad [2\text{-}37]$$

The electrical resistivity of any material is defined as the resistance, in ohms, between opposite faces of a unit cube of the material (Whittington et al.1981). Thus, if R is the resistance in Ω of a block of concrete having a length L (m), and a cross-sectional area, A (m^2), the resistivity, ρ(Ωm), is expressed by the formula,

$$\rho = \frac{RA}{L} \qquad [2\text{-}38]$$

Resistivity, being a fundamental property of the material, is independent of the volume of the specimen, whereas resistance depends upon its shape and size.

Electrical resistivity measurements on concrete can be done by applying either a direct current (DC) or an alternating current (AC) (Hansson et al. 1983). The use of a DC voltage results in polarization of the electrolyte and the formation of hydrogen and oxygen gas at the measuring electrodes (Monofore 1968; Hansson et al. 1983). The polarized layers in the vicinity of the electrodes produce an effective polarization potential known as "back emf". This polarization potential opposes the flow (Monofore 1968) and manifests itself in the form of a reduced current for a given applied voltage, V,

$$R = \frac{V - V_P}{I} \qquad [2\text{-}39]$$

where V_p is the polarization potential, I is the current and R is the electrical resistance across the sample. If it is assumed that this polarization effect is constant at different applied voltages, this effect can be accounted for by taking current measurements at two different applied voltages. The polarization potential is given by (Monofore 1968):

$$V_P = \frac{V_1 I_2 - V_2 I_1}{I_1 - I_2} \qquad [2\text{-}40]$$

where V_1 and V_2 are the two applied voltages and I_1 and I_2 are the corresponding currents.

After analyzing the above two experimental methods, it was decided that the resistivity technique was the more suitable method for determining the dependence of the diffusion

coefficient on saturation of concrete for the following reasons: a) The experimental data could be used to determine the necessary parameters required in models when predicting the transport of chlorides in unsaturated concrete, and b) the experimental set-up is easy and the experiment can be performed in a very short time compared to other experiments.

2.3 Models for Predicting Chlorides Ingress

There are mainly three different approaches to model moisture movement and chloride ions ingress in unsaturated concrete:

1. Diffusion Models;
2. Advection-Diffusion Models; and
3. Multiphase Multicomponent Models.

2.3.1 Diffusion Models

Diffusion models are applicable to concrete structures that are permanently wet. However, they underestimate the amount of chlorides that may penetrate concrete structures subjected to wetting and drying cycles, as is the case of structures exposed to marine environments in the splash and tidal zones or for highway structures exposed to de-icing salts. Chloride profiles in these structures depend strongly on moisture distribution in the concrete cover. Diffusion is a very slow process compared to the advective movement (Peclet number, $P_e > 10$) in unsaturated conditions (Martys 1995, Puyate and Lawrence, 1998).

A large amount of the work done on service life modelling associated with chloride induced corrosion has used diffusion as the main transport mechanism of chloride ions within concrete, under the assumption that the concrete cover is fully saturated. The effect of capillary sorption on chloride diffusion coefficient has sometimes been included in these types of models by modifying the boundary conditions and material properties. However, some researchers (Bazant and Najjar 1972; Saetta et al 1993) have modelled chloride transport in unsaturated concrete by modifying the effective diffusion coefficient through the use of a humidity factor.

Saetta et al. (1993) introduced an empirical relationship wherein the chloride diffusion coefficient decreases with a decrease in the concrete pore relative humidity, as follows:

$$\begin{cases} D_{cl} = D_{eff}\left[f(h) \right] \\ f(h) = \left[1 + \dfrac{(1-h)^4}{(1-h_c)^4} \right]^{-1} \end{cases} \quad [2\text{-}41]$$

where h is the concrete pore relative humidity and h_c is the humidity at which D_{eff} drops halfway between its maximum and minimum values, taken to be 0.75 from the work done by Bazant and Najjar (1971) on drying of concrete.

2.3.2 Advection-Diffusion Models

The advection–diffusion equation is a partial differential equation, which describes physical phenomena where chloride is transferred inside concrete due to two processes: advection and diffusion. The total mass flux can be written as a sum of an advective flux and a diffusive flux. The equation can be derived from the continuity equation, which states that the rate of change of a scalar quantity in a differential control volume is given by flow and diffusion into and out of that part of the system along with any generation or consumption inside the control volume.

Saturated conditions

In its simplest form under saturated condition (when the diffusion coefficient and the advection velocity are constant and there are no sources or sinks) the equation takes the form:

$$\phi \frac{\partial C}{\partial t} = D_{eff} \frac{\partial^2 C}{\partial x^2} - q \frac{\partial C}{\partial x} \quad [2\text{-}42]$$

The two terms on the right hand side represent different physical processes: the first term represents the diffusion flux while the second describes advective flux. The advective flux is caused by the bulk movement of the fluid and the diffusive flux is attributed to the gradient in the solute concentration. Under full saturation, all of the pores are available to transmit a fluid. The advection-diffusion equation expressed in Cartesian coordinates is

$$\phi \frac{\partial C}{\partial t} = D_{eff}\left(\frac{\partial^2 C}{\partial x^2} + \frac{\partial^2 C}{\partial y^2} + \frac{\partial^2 C}{\partial z^2}\right) - \left(q_x \frac{\partial C}{\partial x} + q_y \frac{\partial C}{\partial y} + q_z \frac{\partial C}{\partial z}\right) \qquad [2\text{-}43]$$

where q_x, q_y and q_z are the velocity components in the x, y, and z directions, respectively.

Unsaturated conditions

Unlike the saturated condition, all of the pores are not available to transmit a fluid in the unsaturated condition. In an unsaturated porous medium, the cross sectional area available for flow not only depends on the porosity of the material but also on the saturation of the liquid phase. Therefore, the cross section available for flow is only a fraction of the porosity. The advective-diffusion equation for unsaturated condition takes the form:

$$\frac{\partial(\phi S_l C)}{\partial t} = \frac{\partial}{\partial x}\left(D_{eff} \frac{\partial C}{\partial x} - q_l C\right) \qquad [2\text{-}44]$$

where q_l is the moisture flux given by equation [2-5].

2.3.3 Multiphase Multicomponent Models

The chloride mass balance equation for multiphase multicomponent models can be written similar to equation [2-44], with q_l given by equation [2-16].

As with flow, boundary conditions must be defined to represent solute transport through a boundary value problem. The problem can then be solved to find the distribution of solute mass throughout a domain either numerically or analytically. In order to solve the advection–diffusion equation or multiphase multicomponent models, transport boundary conditions must be defined for the entire boundary of a domain. However, the values and types of boundary conditions may change with time. Often, the most challenging aspect of analyzing flow is the definition of boundary conditions that represent the physical flow system. In some cases, it is not possible to define boundary conditions

based on physical features. In these cases, boundary conditions must be chosen based on an understanding of the effects of such choices on the flow regime being represented.

There are two primary types of boundary conditions that are used to analyze water flow and the transport of chlorides. The first type defines the value of the primary variables, such as pressure, temperature, etc. along the boundary and is known as a Dirichlet boundary condition. The second type of boundary condition defines the gradient of the primary variables and is known as a Neumann boundary conditions. The flux can be defined based on the hydraulic conductivity and the hydraulic head gradient using Darcy's equation or Richard's equation. If the boundary condition is defined based on the water flux, then the hydraulic conductivity of the medium must be defined at the boundaries to determine the gradient.

One of the below two conditions can be applied to define the transport of solutes across a boundary.

1. The concentration can be defined at the boundary as a function of time, forming a type one, or Dirichlet type boundary condition. The boundary condition is of the form:

$$C = C(t) \qquad [2\text{-}45]$$

2. The derivative of the concentration perpendicular to the boundary can be defined as a function of time, controlling the diffusive mass fluxes across the boundary. This forms a type two, or Neumann, boundary condition of the form:

$$\frac{\partial C}{\partial x} = \frac{\partial C}{\partial x}(t) \qquad [2\text{-}46]$$

2.4 Literature Survey Summary

In the case of unsaturated concrete, water flux and, subsequently, the transport of dissolved chloride ions in response to a specified potential gradient are strongly

dependent on the saturation of concrete. Darcy's Law, which has been applied to single phase flow in porous media, can be generalized for unsaturated flow or multiphase flow, with permeability replaced by phase permeability. There has been very little work reported in the literature related to moisture flow and transport of chlorides under unsaturated concrete. Presently, there are no standard test methods for measuring key transport properties of concrete, such as permeability and capillary- driven moisture transfer. However, some test methods developed and used by other disciplines like soil sciences, rock sciences and petroleum sciences should be equally applicable to concrete.

The equilibrium state of water in an unsaturated porous material is characterized by its capillary pressure-degree of saturation function (also known as moisture retention function). There has been very little effort to establish relationships for the capillary pressure as a function of degree of saturation for concrete. In addition to the capillary pressure-saturation function, the relative permeability-saturation function is also necessary for modelling moisture transport in concrete. The direct measurement of relative permeability in concrete is still a challenge and subject of considerable research. Typically, these functions are estimated using water retention and saturated hydraulic conductivity measurements together with the choice of a suitable mathematical model (e.g., Mualem 1976; van Genuchten 1980). Therefore, determination of the moisture retention functions is necessary for the modelling of moisture flow and transport of chlorides in unsaturated concrete. There are two common methods found in the literature for measuring moisture retention data of a porous material in the high capillary pressure range using controlled-suction techniques: the pressure membrane technique and the vapour equilibrium technique. The vapour equilibrium technique is widely used for measuring moisture retention data of concrete and will be used in this research.

In unsaturated concrete, the effective diffusion coefficient is no longer a constant but a function of saturation (Bazant and Najjar 1972; Garboczi 1990; Saetta et al. 1993; McCarter, et al. 2001) and, therefore, can not be described by simple diffusion theories that are typically used in the present literature on concrete. Dependence of the diffusion coefficient on the degree of saturation is essential for determining the moisture flow and

transport of chlorides in unsaturated concrete, in addition to the basic physical properties of concrete e.g. porosity, density, saturated hydraulic conductivity and moisture retention function. Up to now, relatively few authors have focused on the effect of water saturation upon the diffusion coefficient in unsaturated porous materials, despite the fact that this is an essential component needed when modelling the transport of ions under variably saturated conditions. Direct and indirect techniques have been used for measuring diffusion coefficients in porous media. However, due to some practical complexity, such as maintaining proper boundary conditions and the difficulty in experimental setup involved with direct techniques, indirect methods are used to measure diffusion coefficients in unsaturated porous materials of low porosity. The most widely used indirect method is the measurement of electrical conductivity or electrical resistivity, which provides reliable estimates of diffusion coefficients in unsaturated porous materials (Atkinson et al. 1984; Conca and Wright 1990).

Diffusion models are applicable to concrete structures that are permanently wet. However, they underestimate the amount of chlorides penetrating the concrete structures operated under unsaturated condition. Unsaturated flow models and associated solute transport models are widely used for the study of flow and transport processes in porous media under unsaturated conditions and should be applicable to concrete for modelling moisture flow and transport of chlorides under unsaturated conditions.

3 Materials and Methods

Three different experiments were conducted to determine the parameters necessary for modeling moisture flow and the transport of chlorides in unsaturated concrete. Concrete mixes with three different water-cement ratios were used. A centrifuge test was performed to determine the saturated hydraulic conductivity of the concrete. The vapour equilibrium technique was used for determining the moisture retention characteristic of the concrete. A resistivity technique was performed to determine the dependence of the diffusion coefficient on the degree of water saturation.

3.1 Materials and concrete mixtures

Normal Portland cement (CSA A5 Type 10) was used as the cementitious material. Type 10 Normal Portland cement is a general-purpose cement, suitable for all uses where the special properties of other cement types are not required. The chemical composition and mineral composition of Type-10 cement are given in Table 3-1 and Table 3-2.

Table 3-1: Chemical composition of Portland cement (CSA A5 Type 10)

Chemical composition (%)	
SiO_2	20.70
Al_2O_3	3.68
CaO	63.00
Fe_2O_3	2.95
MgO	4.21
Na_2O	0.14
K_2O	0.59
SO_3	2.62
Free CaO	1.02
Loss on ignition	2.70

Table 3-2: Mineral composition of type-10 Portland cement (Canadian Portland Cement Association)

Mineral Composition (%)	
C_3S	*50*
C_2S	24
C_3A	11
C_4AF	8

The raw materials used for the concrete mixes are shown in Table 3-3.

Table 3-3: Raw materials

Material	*Type/ Source*	*Comments*
Cement	Lafarge	CSA A5 Type 10
Coarse Aggregate (5/14 mm)	Lafarge, washed gravel	CSA A23.2-12A Absorption
Fine Aggregate	Pit run, Coarse sand	CSA A23.2-6A Absorption
Water	Tap water	
Superplasticizer	Master Builders, DARCEM-19	ASTM C-494 Type A & F
Air Entrainer	Master Builders-AE 90	ASTM C-260

Three concrete mix proportions, representing a range of water to cement (w/c) ratios, were used for this study. For easy identification, all samples were labelled according to their w/c ratio. All samples from mix-1(w/c ratio=0.4) were designated as A, and similarly from mix- 2 (w/c ratio=0.5) and 3 (w/c ratio=0.6) were designated as B and C, respectively. The mix designs are shown in Table 3-4.

A few days prior to mixing, the coarse aggregates were washed with water to remove dust or other coatings from the surface of the aggregates. The wet coarse aggregate was then immersed in water at room temperature for a period of 24 hours. The aggregate was removed from the water and allowed to partially air dry for about 15 minutes, on an

inclined metal pan to remove the excess surface water. After that, the surface moisture was wiped off using a large absorbent cloth.

Table 3-4: Mix designs

W/C	*0.4*	*0.5*	*0.6*
Portland Cement (kg/m^3)	446	357	298
Coarse Aggregate (kg/m^3)	900	900	900
Fine Aggregate (kg/m^3)	670	750	800
Water (kg/m^3)	178	178	178
Superplasticizer (% by weight of cement)	1.0	0.5	0.0
Air Entrainer (% by weight of cement)	0.35	0.35	0.35

A power-driven upright mortar mixer was used for the mixes. The superplasticizer was pre-blended with the mix water. The coarse aggregate was placed first in the mixer and some of the mixing water was added to it. The mixer was started and then the fine aggregate, cement, and water were added with the mixer running. Once all the ingredients were in the mixer, the concrete was mixed for 3 minutes, followed by a 3 minutes rest, followed by 2 minutes of final mixing. An air entrainer was evenly added during the 2 minutes of final mixing. To eliminate segregation, the machine-mixed concrete was placed on a damp mixing pan and remixed by shovel until it appeared to be uniform. At the end of the mixing, the slump and air content of the mix were measured in accordance with CSA standard A23.2-5C and A23.2-7C, respectively. The concrete mixes were then introduced and vibrated in cylindrical moulds (Φ 75x150 mm). All the cylindrical moulds were placed under water-soaked burlap and a plastic sheet in the concrete lab for initial curing. After 24 hours, the concrete cylinders were demolded, labelled and submerged in a saturated lime water tank at room temperature for 27 more days. Keeping the samples in saturated lime water prevented lime from leaching out of the concrete. Saturated lime water can be obtained by dissolving 1.5 g of $Ca(OH)_2$ in one

litre of tap water. To prevent carbonation, concrete samples were stored in lime water until testing.

The properties of the fresh concrete used in the present study are shown in Table 3-5.

Table 3-5: Properties of fresh concrete

W/C	*0.4*	*0.5*	*0.6*
Slump (mm)	59	58	61
Air Content (%)	6.4	6.6	7.8
Density (kg/m^3)	2420	2390	2340

The compressive strength was measured at 28 days. Three 75 mm diameter150 mm long cylinders from each concrete mix were tested for compression by loading the saturated specimens. The cylinders were capped with sulphur shortly before they were tested to avoid any stress concentration, as shown in Fig. 3-1. The sulphur was applied in a molten state and allowed to harden with the specimen in a jig which ensured a plane and square ended surface. The diameter of the cylinders was measured at five different places and the average diameter was used to calculate the average area of the cylinder. The ultimate failure load and average area were used to determine the compressive strength of the concrete cylinders.

Porosity of the concrete samples was measured in accordance with ASTM C 642-97. Table 3-6 shows the porosity and compressive strength values of three concrete mixes. Both the porosity and compressive strength values given in Table 3-6 are the average of three concrete samples from similar mixes at 28 days.

Table 3-6: Properties of concrete at 28 days

W/C	*0.4*	*0.5*	*0.6*
Porosity (%)	11.56	12.19	13.10
Compressive Strength (MPa)	41.75	37.63	31.76

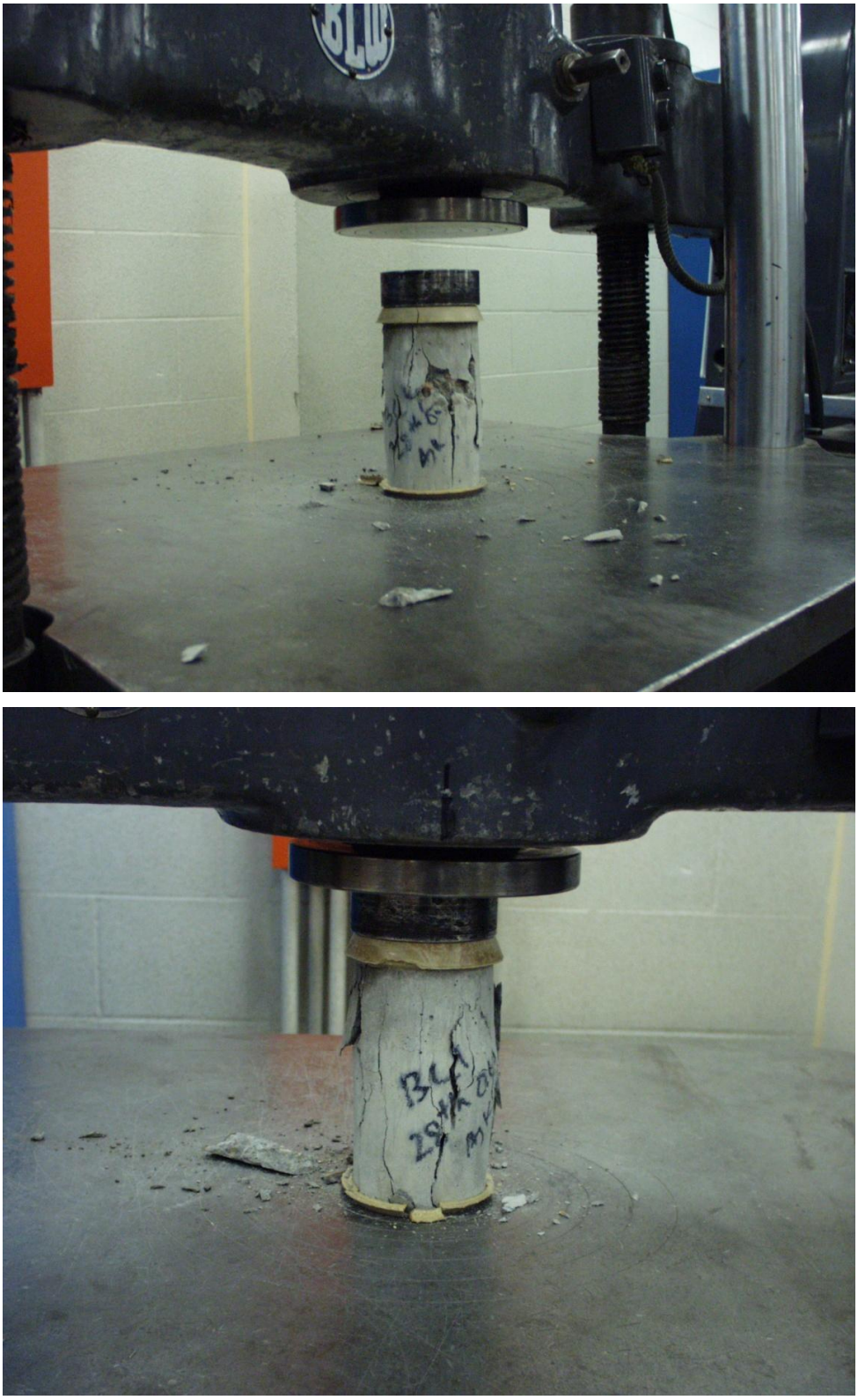

Figure 3-1: Concrete compressive test setup.

3.2 Centrifuge Technique

The centrifugation technique was used to determine the saturated hydraulic conductivity of the concrete samples. Centrifugation provided a very large driving force which reduced the experimental time significantly. The other advantage of using a centrifuge is that the centripetal force exerted by a centrifuge is a body force similar to gravity and acts simultaneously over the entire system and independently of other driving forces such as gravity (Conca and Wright 1990). The schematic representation of a concrete sample in the centrifuge is shown in Figure 3-2

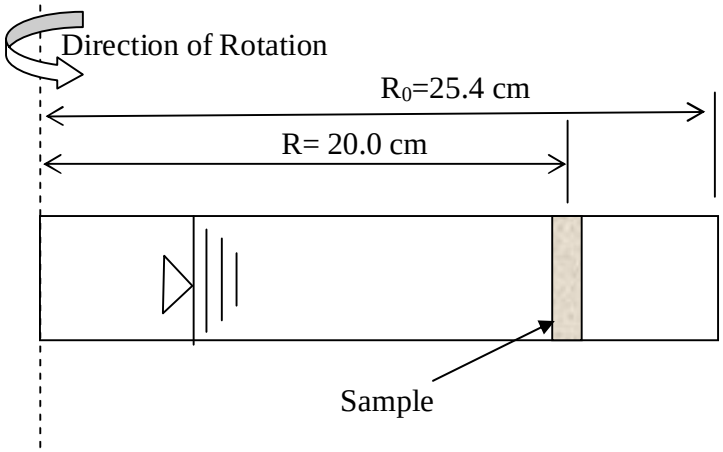

Figure 3-2: Schematic representation of a concrete sample in a centrifuge.

3.2.1 Equipments and Materials

Details of the geotechnical centrifuge used for this study are presented in Table 3-7.

Table 3-7: Details of the centrifuge

Type	Swinging buckets on both sides of the arm
Model	J6-HC Centrifuge- Beckman Coulter
Rotor	JS-4.2 swinging bucket
Operative arm radius	190 mm
Maximum radius	254 mm
Centrifugation angular velocity	800-900 rpm
Maximum angular velocity	4200 rpm

The JS-4.2 rotor assembly of the centrifuge consists of six swinging type buckets capable of carrying six test specimens in one test run (Figure 3-3). The buckets in the centrifuge can be subjected to angular velocities varying from 50 to 4200 rpm. The swinging buckets of the centrifuge assume horizontal positions when the centrifuge is spinning. All of the six buckets can be used simultaneously with six specimen holders for testing. The combined mass of the specimen, the holders and the buckets should be equal to avoid rotary imbalance. Specially designed concrete specimen holders (Figure 3-4) were constructed and used with already available soil specimen holders (Figure 3-5) to accommodate the specimens in the two-centrifuge bucket, placed diagonally opposite to each other.

Figure 3-3: Centrifuge rotor assembly with six swinging type buckets.

Most permeability tests require the application of high pressures due to the relatively low permeability of concrete. However, when high pressures are used to overcome the low flow problem, sealing around the sample becomes quite difficult. When concrete samples are rotated at very high speed in the centrifuge, the samples experience an outward force. This, in turn, demands efficient surface sealing of the samples parallel to the direction of flow. Numerous sealers available in the lab were tried but none of them were able to prevent leakage above 400 rpm centrifuge speed. Finally, Dow Corning ®

888 silicon joint concrete sealant was tried and used. It is a ready-to-use one-component silicon rubber which meets the requirements of ASTM D5893 Type NS. To verify that there was no leakage through the sealant, an acrylic disc was used in the sample holder in the place of the concrete sample. Tests were run three times, each lasting for an hour, with the acrylic disc. The disc was centrifuged up to an angular velocity of 1200 rpm in all the three test runs. The water level in the water tube of sample holder remained constant during each of the three tests, which confirmed that there was no leakage of water through the sealant when the angular velocity of centrifuge was less than 1200 rpm. Even though there was no leakage up to 1200 rpm, it was decided that the entire test would be performed below an angular velocity of 1000 rpm even though the maximum angular velocity of the centrifuge is 4200 rpm.

Sample Holder

Two acrylic concrete sample holders, which can hold 13 mm thick concrete samples, were specially designed to apply the principle of the falling head permeability method using a centrifuge. Figure 3-4 shows a typical acrylic concrete sample holder used in this study. The concrete sample holders were designed such that they could be used easily with already available aluminum soil holders. The inner diameter of the water tube of concrete holder was kept small so that even low flow rates of water through the sample could be accurately measured. In addition to the silicon sealant, a rubber O-ring was used to keep the sample in position and also to prevent water leakage along the sides of the sample. The sealant was used over the full depth of the concrete specimen. A gap of 1-2 mm was always maintained between the concrete sample and water tube of the sample holder to make sure that the water was in contact with the full surface area of the concrete sample during the test, as shown in Figure 3-4.

Sample preparation

Samples of diameter 50 mm were cored from concrete cast as 75 mm diameter150 mm long cylinders. The mix designs used are shown in Table 3-4. All the samples were cast as explained in Section 3.1. After 45 days of curing, 12.5 mm thick disks were cut from the

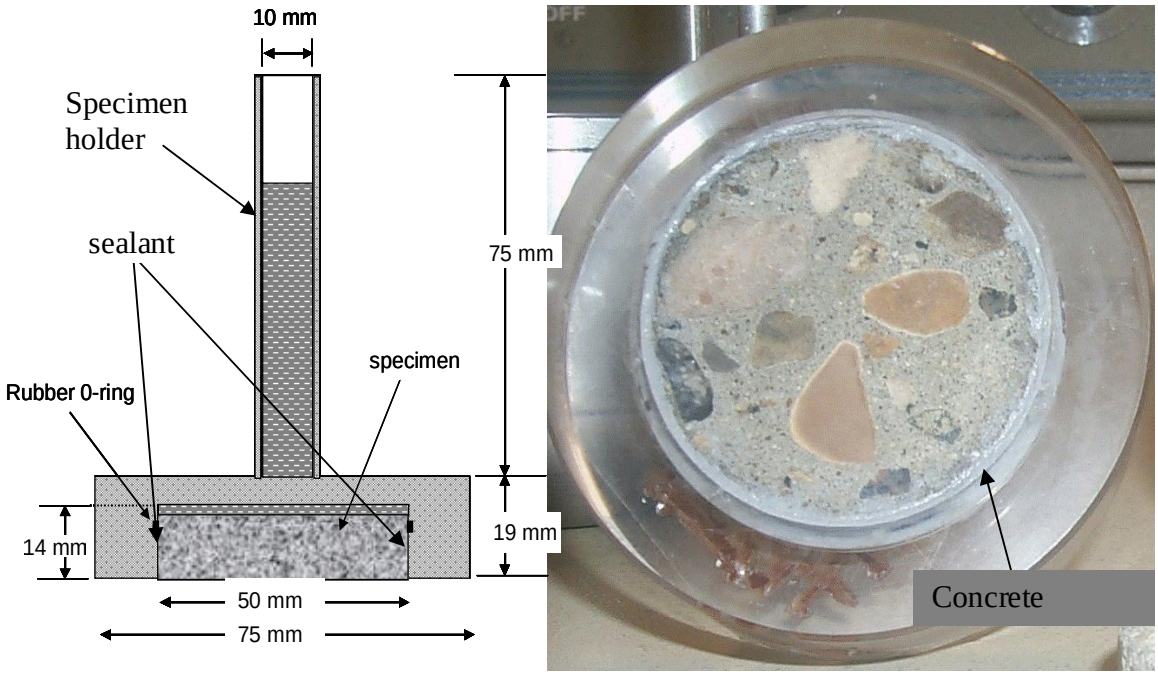

Figure 3-4: Concrete sample holder

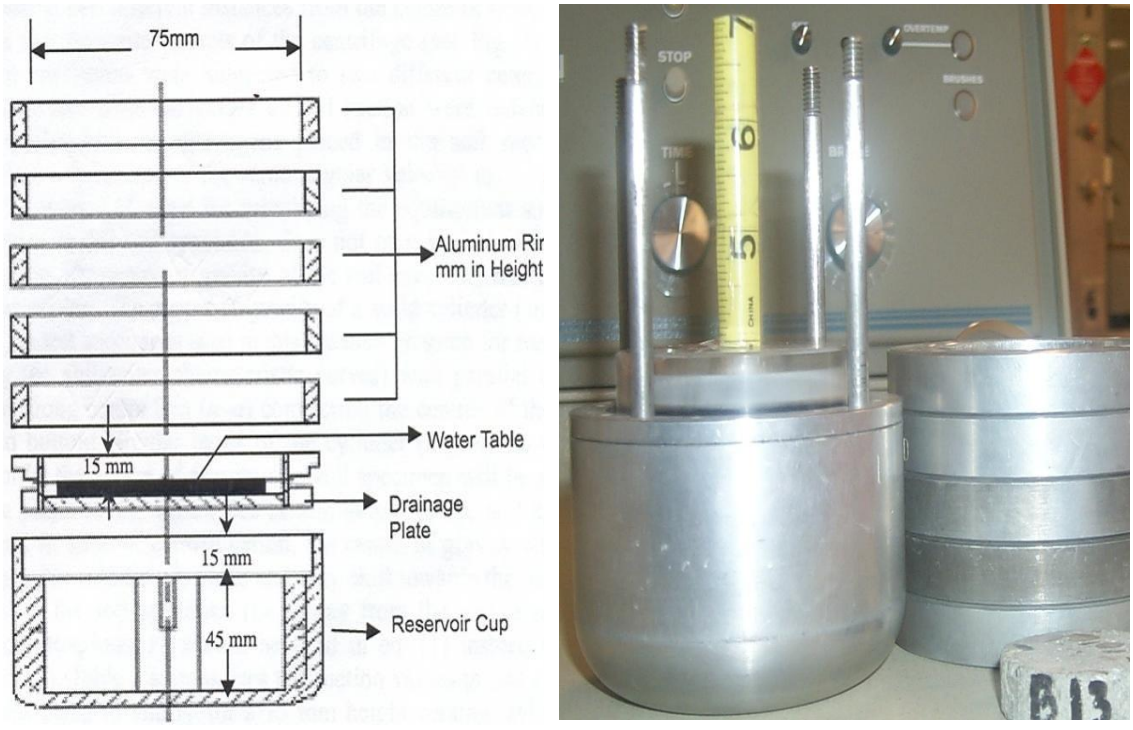

Figure 3-5: Soil sample holder (a) Details of the aluminum soil holder (Khanzode, 2002) and (b) concrete sample holder used with aluminum soil holder.

cored samples using a diamond saw with water as a coolant. Cooling with water minimizes the risk of drying the specimen during sawing.

3.2.2 Testing Method

At the start of each test, the circumferences of each concrete sample, as well as the inside of the sample holder, were coated with the sealant before inserting the sample into the sample holder. The sealant was allowed to cure overnight. After that, the concrete sample holder, with the sample sealed inside was placed inside the aluminium soil sample holder, as shown in Fig. 3-5 (b). The water tube of the concrete holder was filled with water and the top of the water tube was covered with an aluminium foil to prevent any moisture loss by evaporation. When the sample tube was filled with water, it was ensured that all the air bubbles between the concrete sample and the tube were eliminated. The initial height of the water in the tube was also noted. The weight of the concrete sample holder with the concrete specimen sealed and the water tube filled was determined at the start of each experiment. All experiments were conducted at 23 ± 0.5°C by setting the temperature of the centrifuge at 23°C. Both aluminium soil holders were then placed in the centrifuge bucket.

The pairs of samples were centrifuged at speeds ranging from 800-900 rpm for nearly 25-30 hours until a sufficient number of data points were collected. Samples from concrete mixes with w/c ratios of 0.5 and 0.6 were centrifuged at 800 rpm while samples from the concrete mix with w/c ratio of 0.4 were centrifuged at 900 rpm. The higher angular velocity of centrifugation for a w/c ratio of 0.4 was chosen to keep the experimental time short since, depending upon the porosity and water contents, different periods of time are required for hydraulic equilibrium. To make sure that the sample was fully saturated during the test, not only the initial and final water level in the water tube was measured, but also the initial and final weight of sample holder with concrete specimen and water was measured after every centrifuge run. Only those values where the loss of water in the water tube was equal to the difference in weight of the sample holder set up were considered for the results. Water coming out of the concrete samples was collected in the reservoir cup of the sample holder. In some cases, when there were

invisible minor cracks in the sample or when the samples were not properly sealed, the water tube emptied within an hour of centrifugation. Cracked samples were discarded and poorly sealed samples were resealed. Due to the very low saturated hydraulic conductivity of concrete, it is reasonable to assume that even a slow leak could make a significant difference in the measured saturated hydraulic conductivity of concrete. Keeping this fact in mind, the cross sectional area of the water tube of concrete sample holder was designed to be very small to make sure that even a small water leak should make a significant difference in the conductivity calculation and get noticed easily. None of the samples, except the samples already discarded or resealed, showed any indication of even a slow water leak.

For every pair of samples, during its 25-30 hours of experimental time period, the centrifuge was stopped nearly five to six times to get a number of data sets. Each data set consisted of initial and final level of water in the water tube, centrifugation time, and initial and final weight of concrete sample holder set up. The diameter-length of the samples was measured at three locations by means of dial gauge and the average value was used for calculations.

Once the hydraulic conductivity measurements were taken on a pair of samples, the samples had to be taken out of the concrete sample holder without damaging either. This was done safely by centrifuging the concrete sample inside the sample holder at an angular velocity higher than 1500 rpm. The concrete seal broke at that speed and concrete samples came out easily without any damage.

3.3 Vapour Equilibrium Technique

The basic tools for a good understanding, quantification and prediction of moisture movement in concrete are provided through water vapour desorption and adsorption isotherms. In order to obtain such curves, a vapour equilibrium technique was used. The experiments were carried out on three different concrete mixes at a constant temperature at 22±0.5°C. The vapour equilibrium technique was used so that suction pressures ranging from 3 to 1000 MPa could be created, using salt or acid solutions. The principle of this technique was discussed in section 2.1.3.

3.3.1 Equipments and Materials

The three different concrete mixes used for sample preparations are shown in Table 3-4. Concrete cylinders 75 mm in diameter and 150 mm in length were cast from concrete mixes, as explained in section 3.1, and cured for 45 days in saturated lime water. The cylinders were cured for 45 days to minimize the water loss due to the cement hydration process during the long duration of the experiments. The water loss due to the cement hydration process can therefore be assumed to be negligible during the experiments. After 45 days, the cylinders were taken out of the lime bath and 50 mm diameter concrete cylinders were cored from them. This was done to avoid any possible skin effect during the experiments. The samples, 12 mm in thickness and 50 mm in diameter, were then wet-sawed from the cored concrete cylinders. The 12 mm thick discs were used to obtain moisture equilibrium reasonably quickly.

Twelve different desorption environments, ranging from RH = 8.2 to 97.3 %, were imposed on concrete samples by using twelve different salts for this study. The desorption environments were created by means of saturated salt solutions, kept in closed containers at normal room temperature (22±0.5°C), as shown in Figure 3-6. Table 3-8 shows the saturated salt solutions used and the corresponding equilibrium relative humidity environment (European Standard 1996; Waxler 1954) when pure salt and distilled water is used.

The relative humidity created by a saturated salt solution depends upon the quality of salt and water used. The function of a saturated salt solution is to create a specific humidity condition by giving off or absorbing moisture from the vapour space above it. Any porous material present in the environment will absorb or give off moisture and may cause a shift in the equilibrium relative humidity condition (Labuza 1963).

a)

b)

Figure 3-6: (a) Relative humidity environment created inside the lab, and (b) Relative humidity and Temperature measurement using Humidity probe.

Therefore, a relative humidity probe with an accuracy of ± 1% previously calibrated with saturated salt solution over the range 10%-100% was used to measure the actual RH inside the humidity boxes. The salt solutions were prepared as per European Standard (ISO/DIS 1257 1996).

Table 3-8: Relative humidity and total suction (MPa) values of different salts used

Symbol	Salt	RH	Total Suction(MPa)
1	Potassium Sulphate	97.3	3.7
2	Potassium Nitrate	93.5	9.2
3	Potassium Chloride	84.3	23.3
4	Ammonium Chloride	78.5	33.0
5	Sodium Chloride	75.3	38.6
6	Potassium Iodide	68.9	50.8
7	Sodium Bromide	57.6	75.2
8	Potassium Carbonate	43.2	114.4
9	Magnesium Chloride	32.9	151.9
10	Potassium Acetate	22.5	203.3
11	Lithium Chloride	11.3	297.1
12	Sodium Hydroxide	8.2	340.8

3.3.2 Testing Method

At the start of the experiment, saturated salt solutions were prepared from twelve different salts as mentioned in the Table 3-8. The salt solutions were prepared in the environmental laboratory under the guidance of an experienced technician due to the high corrosiveness of some of the salts. It was ensured that there were always some excess solid salts in the saturated solution. In total, 36 wide mouth acrylic square bottles were used as humidity chambers. The square bottles contained the saturated salt solutions. In order to avoid any misplacement of samples, all the bottles were labelled. The first part of the label represented the type of concrete mix and the second part represented the type of salt solution, as shown in Figure 3-6. In order to obtain values

representative of the concrete material, it was decided that three samples would be used for each relative humidity boundary condition from each of the concrete mixes. Four holes were made in the cap of each bottle; three for suspending the samples and the forth for inserting a relative humidity probe inside the bottle for measuring the actual RH during the experiment. It was found during the set up that suspending the samples separately was not convenient. Therefore, it was decided that the samples would be suspended together. Now, since only two out of the four holes in the cap were necessary during the experiments; one for suspending the three tied samples and other for inserting the humidity probe; the other two holes were sealed using rubber stoppers.

Concrete samples were taken out of the lime bath and the excess surface moisture was dried by wiping the samples with tissue paper. The weight of the samples, initial saturated surface dry (SSD) weight, m_s, were recorded and samples were temporarily submerged in lime baths. The mass of all the samples was measured to the nearest 0.001 gm. Three samples from each mix type were taken and tied together using copper wire for each humidity boxes. Copper was used for wire material simply to avoid rusting due to water condensation at its surface, inside the humidity boxes. In addition, the samples were separated from each other using O-rings having diameter much less than that of the exposed surface area of samples. The use of O-rings kept the side faces of the samples apart and at the same time provided a sufficient gap between the samples for air circulation. The tied samples were then suspended, for desorption, inside the humidity boxes using copper wire and rubber stoppers. Figure 3-7 shows the way the samples were tied together and suspended inside the humidity boxes. It was ensured that suspended samples were not in contact with the salt solution directly.

The water content of the samples was monitored by weighing the suspended samples, copper wire and rubber stopper together every 3 days until the weight became stable. The weighing was necessary to know the attainment of equilibrium during the desorption process. Relative humidity and temperature inside the boxes were also measured before taking the samples out for weighing each time. Weighing of the tied samples was done within 15 s of samples being taken out of the boxes. This procedure

was quick enough that any water evaporation during the weighing process could be neglected.

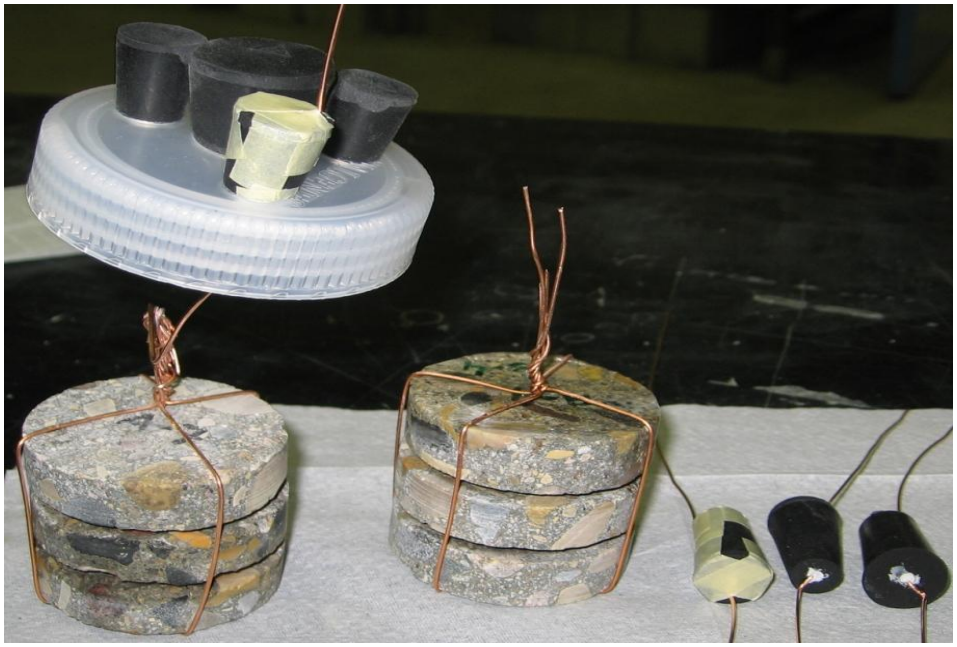

Figure 3-7: Concrete samples used to determine moisture retention function.

Equilibrium was assumed to be reached when the mass loss did not exceed 0.001 gm over a week period. Although the samples in higher relative humidity environments reached equilibrium within two weeks, the samples were kept inside the relative humidity boxes for 28 days. Upon reaching the equilibrium, the samples were taken out of the chamber and the equilibrium weight of the samples, m_h, was measured. The samples were then oven dried at 105 °C for 24 h in order to measure their dry weight, m_d. The degree of water saturation of the samples was then determined using equation [2-13].

3.4 Resistivity Test

The resistivity technique using DC voltage was used to characterize the effect of the degree of saturation on the effective diffusion coefficient. In unsaturated porous materials, the diffusion coefficients of ions depend on the degree of water saturation, as discussed in Section 2.2.3. The effect of degree of water saturation on the diffusion coefficient is an essential parameter needed for modelling the transport of ions under unsaturated conditions. The most widely used indirect method is the measurement of electrical conductivity, which provides reliable estimates of diffusion coefficients (Atkinson et al. 1984; Garboczi 1990; Conca and Wright 1990).

3.4.1 Equipments and Materials

The three different concrete mixes used for sample preparations are shown in Table 3-4. Concrete cylinders 75 mm in diameter and 150 mm in length were cast from concrete mixes as explained in Section 3.1 and cured for 60 days in saturated lime water before testing. The 60 days of curing period was selected considering that most of the cement hydration ceases by this time. After 60 days, concrete samples, 25 mm in height and 75 mm in diameter, were cut from the concrete cylinders.

In order to obtain values representative of concrete material, three samples were tested from each concrete mix. To measure the resistivity with accuracy, it is essential that the current traverses the full area of the samples, and this was ensured by using external brass plate electrodes (diameter 75 mm) of the same shape as the surface of the samples. The surface of the brass plates was made smooth by machine filing. The external brass plate electrodes were placed at opposite faces of the specimens as shown in the Figure 3-8. A G-clamp was used to secure the electrodes to the specimens. A cement paste of water-cement ratio 0.5 was used to ensure intimate contact between the electrodes and concrete specimens. Using cement paste makes the resistivity measurement of concrete specimens more accurate without affecting the resistance being measured since the paste has a very low resistivity (2 Ωm) in comparison to the concrete resistivity (Whittington et al. 1981). The brass plate and cement paste combination ensured a uniform

distribution of current across the surface of the specimen. Before testing, the samples were surface-dried by wiping off any moisture present on the surface with a towel, to ensure that there were no surface conduction effects and that the resistance measured was the volume resistance. Direct current was used for determining the electrical resistivity of concrete samples. The electrical resistance of the samples was measured using a commercially available ohm-meter.

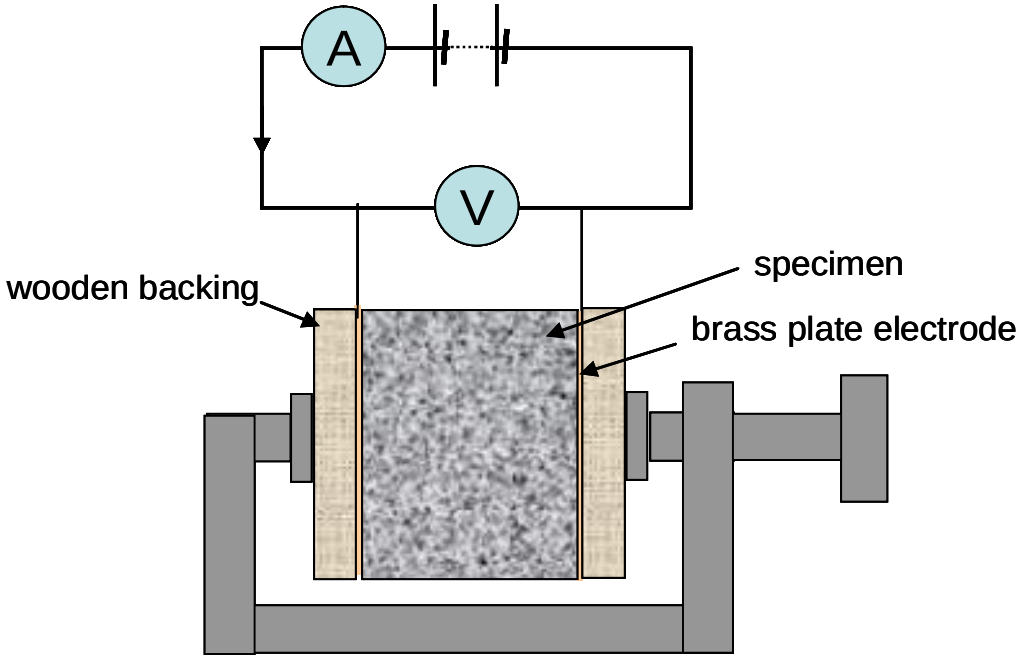

Figure 3-8: Schematic diagram of resistivity measurement.

3.4.2 Testing Method

Initially saturated, surface dry (SSD), weights, m_s, of the samples were measured and samples were temporarily submerged in lime baths. All samples were weighed to the nearest 0.001 gm. Samples were then placed in an oven and dried at 50 °C for different periods of times, ranging from 0.5 h to 48 h, to create different degrees of saturation inside the samples. The samples were then removed from the oven and covered with cellophane and aluminium paper before placing them in watertight bags. The samples were kept in the bag for the time equal to its drying time in the oven. That was done to make sure that the samples had a uniform saturation throughout the depth (Carcasses et

al. 2002). It can be assumed that a good saturation state uniformity had been achieved, accounting for the slow drying process, due to step-by-step drying, the relatively small specimen thickness and the lack of mass loss during the water redistribution period.

The samples were taken out of the bag and weighed ($m_{h)}$ just before measuring the resistance. Each electrical resistivity measurement took about 3-4 minutes and that was the only time when samples came in contact with the environment. The measurement time was so short that it can be safely assumed that the saturation of the samples remained essentially the same during testing. At the end of the experiment, all samples were oven dried at 105 °C for 24 hours in order to measure their dry weight, m_d. The degree of water saturation of the samples was then determined using equation [2-27].

Two different voltages, 5.0 V and 2.5 V, were applied on each sample and the current, I, corresponding to each voltage was measured. The currents were allowed to decay to a steady state value before measuring. The decay time was in the order of a few minutes. The polarization potential was calculated for each set of measurements using equation [2-40]. Once the polarization potential was known, the resistance was obtained using equation [2-39]. The use of higher voltage levels was avoided since higher voltage produces heat during measurement that could change the saturation of the specimens. It is noted that the voltage levels (5.0 V and 2.5 V) were all above the level of polarization potential drop, which is typically ~ 1.5 V. The electrical resistivity of the specimens was calculated using equation [2-38].

3.5 Summary

Three different experiments were performed for determining the saturated hydraulic conductivity, moisture retention function and saturation dependence of the effective diffusion coefficient of concrete. The experiments were carried out on samples prepared from three different concrete mixes; w/c ratio 0.4, 0.5 and 0.6. The physical properties of the concrete mixes were determined experimentally.

A centrifugation technique was used to determine the saturated hydraulic conductivity of the three concrete mixes. A geotechnical centrifuge was used for centrifugation. The experiment was carried out on twelve concrete samples; four from each concrete mix. Using this technique the saturated hydraulic conductivity measurements were made reasonably quickly.

A vapour equilibrium technique was used for determining moisture retention function of concrete. The experiments were carried out on three different concrete mixes at the constant temperature of 22 ± 0.5°C. Twelve different desorption environments were imposed on concrete specimens by using twelve different saturated salt solutions kept in closed containers. The degree of water saturation of the samples was determined at the end of the experiment.

The resistivity technique was used to characterize the effect of the degree of saturation on the effective diffusion coefficient. DC voltage was used for determining the electrical resistivity of concrete. Three samples were tested from each concrete mix. Two different voltages, 5.0 V and 2.5 V, were applied on each sample at different degrees of water saturation. The degree of water saturation of the samples and currents corresponding to each voltage were measured during the experiment.

4 Results and Discussion

4.1 Centrifuge Technique

Saturated hydraulic conductivity was obtained using a centrifuge technique. Twelve concrete samples were used to determine the saturated hydraulic conductivity for three different concrete mixes.

4.1.1 Measurement of Saturated Hydraulic Conductivity

Tests were conducted on 12 concrete samples, 4 samples from each concrete mix. The primary data consisted of the initial and final level of water in the water tube, centrifugation time, centrifugation angular velocity, cross sectional area of concrete sample, cross sectional area of the water tube of concrete sample holder and the length of the sample parallel to the direction of flow. Knowing all the parameters, the values of saturated hydraulic conductivities were obtained using equations [2-23], [2-24] and [2-25]. The results of all the centrifugal analysis are given in Table 4-1.

The largest coefficient of variation of measured saturated hydraulic conductivity is 11.1%, which indicates that the centrifugal technique has the potential for yielding reliable estimates of the saturated hydraulic conductivity in a very short period of time as compared to other standard methods.

Figure 4-1 shows a comparison of the saturated hydraulic conductivity values of twelve different concrete samples. One can easily see that the saturated hydraulic conductivity of concrete depends on the the w/c ratio. The data was characterized by a gradual increase in the saturated hydraulic conductivity as the w/c ratio increased.

Table 4-1: Saturated hydraulic conductivity data of concrete

w/c ratio	0.4	0.5	0.6
Centrifuge frequency (rpm)	900	800	800
Centrifuge angular velocity (rad/s)	94.2	83.8	83.8
Centrifuge acceleration (a)(m/s^2)	1776.5	1403.7	1403.7
N(=a/g)	181	143	143
Mean Hydraulic conductivity of model (K_m)(m/s)	1.6E-09	4.5 E-09	8.3E-09
Mean Hydraulic conductivity of sample ($K=K_m/N$)(m/s)	9.0E-12	3.1E-11	5.9E-11
Minimum Hydraulic conductivity (m/s)	8.2E-12	2.9E-11	5.0E-11
Maximum Hydraulic conductivity (m/s)	9.5E-12	3.3E-11	6.5E-11
Standard Deviation (m/s)	5.4E-13	1.5E-12	6.5E-12
Sample Variance (m/s)	2.9E-25	2.2E-24	4.2E-23
Coefficient of variation	6.0 %	4.7 %	11.1 %

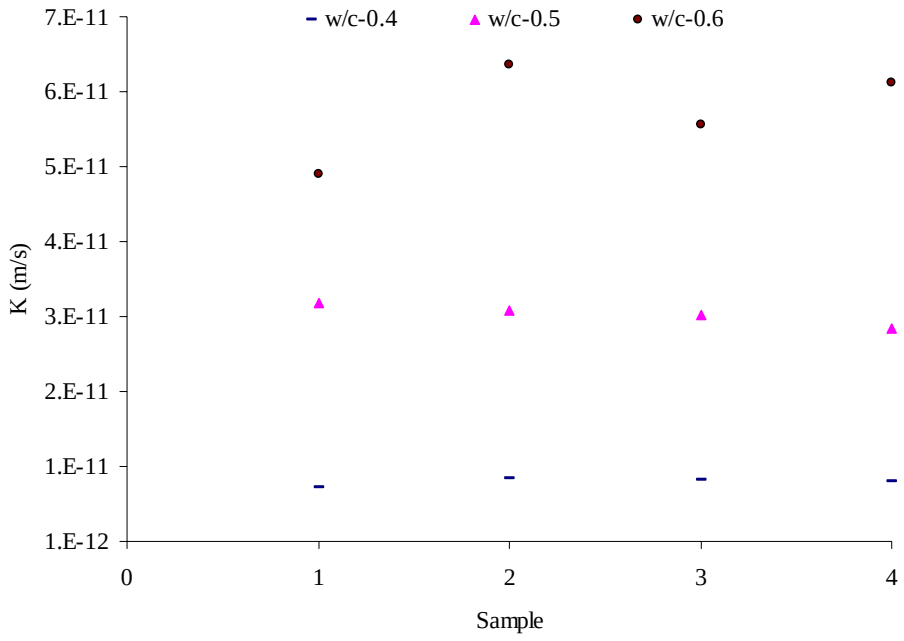

Figure 4-1: Saturated hydraulic conductivity of concrete with w/c ratios of 0.4, 0.5 and 0.6.

To reflect the effect of w/c ratio on the saturated hydraulic conductivity of concrete the measured saturated hydraulic conductivity data were converted to normalized saturated hydraulic conductivity with respect to the saturated hydraulic conductivity of concrete with a w/c of 0.4. Figure 4-2 shows the normalized saturated hydraulic conductivity of three different concrete mixes. The results in Figure 4-2 showed that an increase in the water-cement ratio from 0.4 to 0.6 increased the saturated hydraulic conductivity by almost seven times.

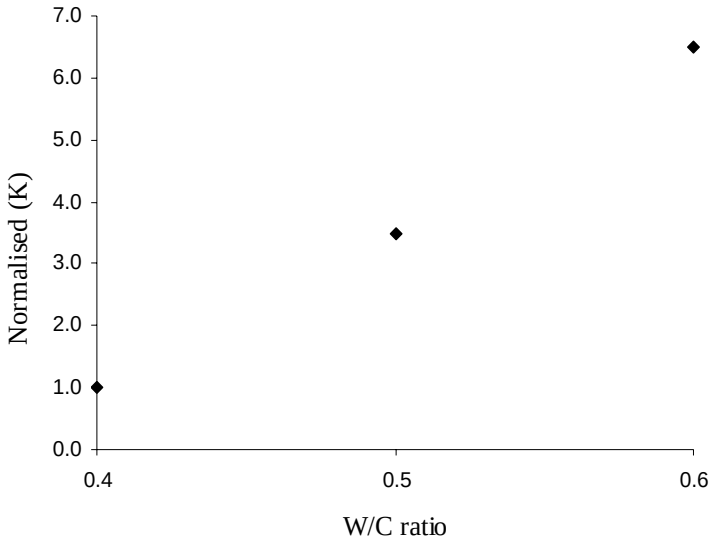

Figure 4-2: Normalized saturated hydraulic conductivity of concrete with respect to w/c ratio.

4.2 Vapour Equilibrium Technique

Moisture retention functions were obtained using the vapour equilibrium technique for three different concrete mixes. In addition, van Genuchten parameters were determined for capillary pressure-saturation and relative permeability-saturation functions, over the entire saturation range. The measurements were conducted only on drained samples.

4.2.1 Moisture Retention Function

Thirty three samples from each concrete mix type were tested in eleven different relative humidity environments. Average values of the saturation from the three identical samples were used for a given relative humidity (RH) condition. The conversion from RH to capillary suction was obtained by using equation [2-26]. Figure 4-3 shows the variation of degree of water saturation with relative humidity (also known as sorption isotherm) for three different concrete mixes. The water saturation of the specimens tested varied in the range of 0.1 to 0.92. The results in Figure 4-3 showed that the degree of saturation decreased with decreasing RH.

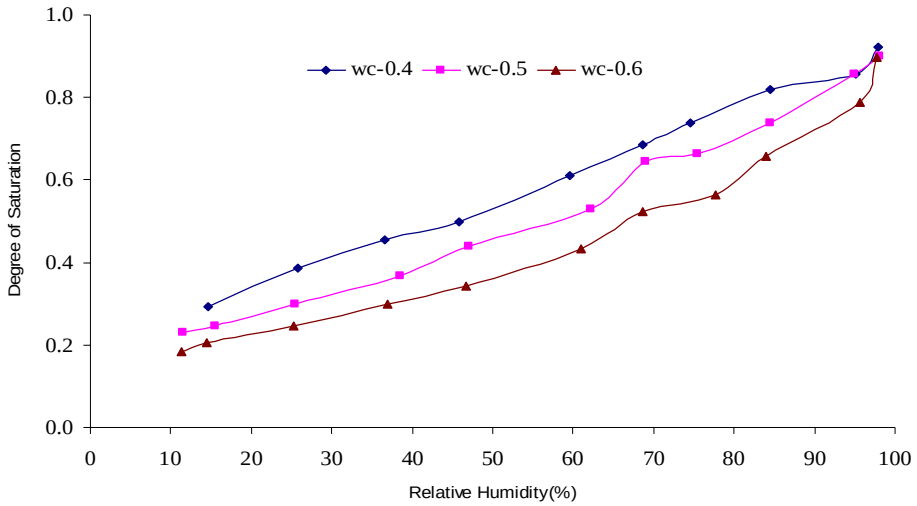

Figure 4-3: Desorption isotherm of concrete mixtures.

The results in Figure 4-3 showed that for a given relative humidity boundary condition, the degree of saturation was higher for the samples with lower w/c ratios. That could be

attributed to a reduced porosity and smaller pore sizes, which makes desorption more difficult. In general, the form of the functional relationship between degree of saturation and RH was slightly non-linear. The results in Figure 4-3 also showed that an increased w/c ratio increased the non–linearity of the functional relationship.

The moisture retention characteristics or the variations of the degree of saturation at different capillary suction are shown in the Figure 4-4 for the three concrete mixes. The results showed that capillary suction strongly depended on the degree of saturation and the w/c ratio of the concrete. The relationship was characterized by a gradual increase in capillary pressure as degree of saturation decreased at higher degrees of saturation, followed by a steep increase at lower degree of saturation. Similarly shaped profiles were obtained for all the concrete mixes. It is evident from Figure 4-4 that, at a given capillary suction, the degree of saturation was higher for the samples with lower w/c ratios. This could be attributed to the presence of smaller size of pores in lower w/c ratio concrete mixes which require larger suction pressures to desaturate. In general, the functional relationship between capillary suction and degree of saturation was non-linear.

Moisture retention in concrete exhibits hysteresis that is., the observed degree of saturation at a given capillary suction depends on whether the concrete is being wetted or dried. However the data on which the parameters of hysteresis could be estimated was not measured due to the inability to carefully control wetting. In general, hysteresis is important only near the cover region where the degree of saturation changes with time is the largest (Meyer et al. 2004).

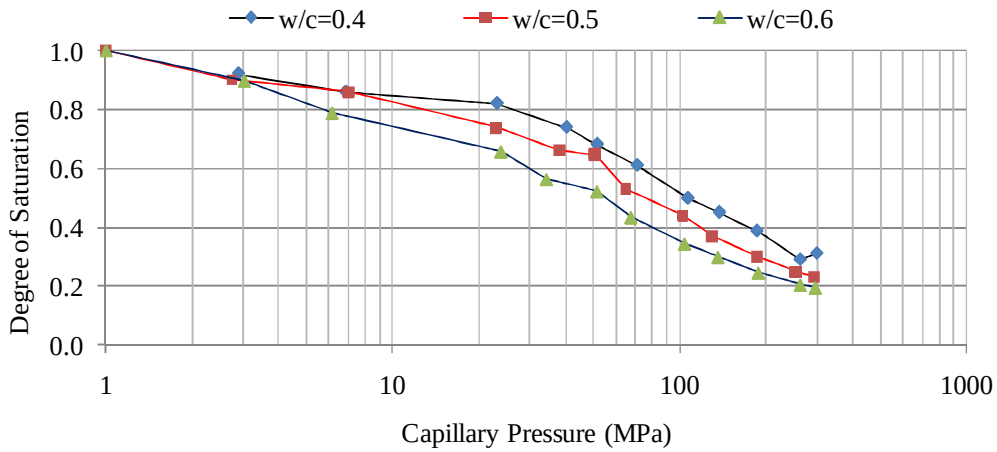

Figure 4-4: Moisture retention curves for concrete mixtures.

Water retention data is typically represented in simulation codes using one of a number of water retention models that have been presented in the literature. In this thesis, the model proposed by van Genuchten (1980) is used. Parameters in the model are as defined for the moisture retention function and can be estimated using moisture retention data.

The experimental moisture retention data was used to determine van Genuchten parameters for each concrete mix type. The retention parameters m and α were fitted to water retention data using the nonlinear, least square, curve-fitting program known as RETC (van Genuchten et. al. 1991). The van Genuchten parameters α and m were obtained for each concrete mix type and are presented in Table 4-2. No standard method for defining residual saturation could be found in the present literature in the case of concrete. The residual water saturation is interpreted here as an empirical parameter and, thus, is generally a fitted parameter. The residual saturation of the concrete mixtures was taken as 0.2. In real field conditions, concrete seldom achieves residual state and therefore this value is not of much importance.

Table 4-2: van Genuchten parameters

w/c	α (1/MPa)	m	S_{lr}	S_{ls}
0.4	0.03494	0.3455	0.2	1
0.5	0.05174	0.3371	0.2	1
0.6	0.0904	0.3248	0.2	1

A “closed-form” analytical expression of the moisture retention function is very important for modelling unsaturated flow of moisture and transport of chlorides in unsaturated concrete. The van Genuchten parameters determined above can be used to determine a capillary pressure-saturation relationship and the relative permeability-saturation over the entire saturation range. A comparison between the van Genuchten model and the experimental capillary pressure-saturation data for all the three concrete mixes is shown in Figure 4-5. Each curve in Figure 4-5 is a graphical representation of the van Genuchten function (1980) defined by equation [2-18]. Since it was necessary for the fitted curves in Figure 4-5 to pass through zero, the resulting van Genuchten model do not reflect the true capillary conditions at some experimental data points. At low degrees of saturation, the van Genuchten model provided a poor representation of capillary pressure. This kind of poor representation has been reported by some other researchers (Meyer et al. 2004; Khaleel et al. (1995), as well.

When the van Genuchten parameters for concrete are compared with those of soil, an important difference concerning “α” is noticed between concrete and soil. The “α” value for concrete is about four orders of magnitude higher than that of soil. This could be explained by the significant difference between the microstructure of concrete and that of soils, as characterized by porosity, distribution of pore size diameter, tortuosity, connectivity and fineness of pores.

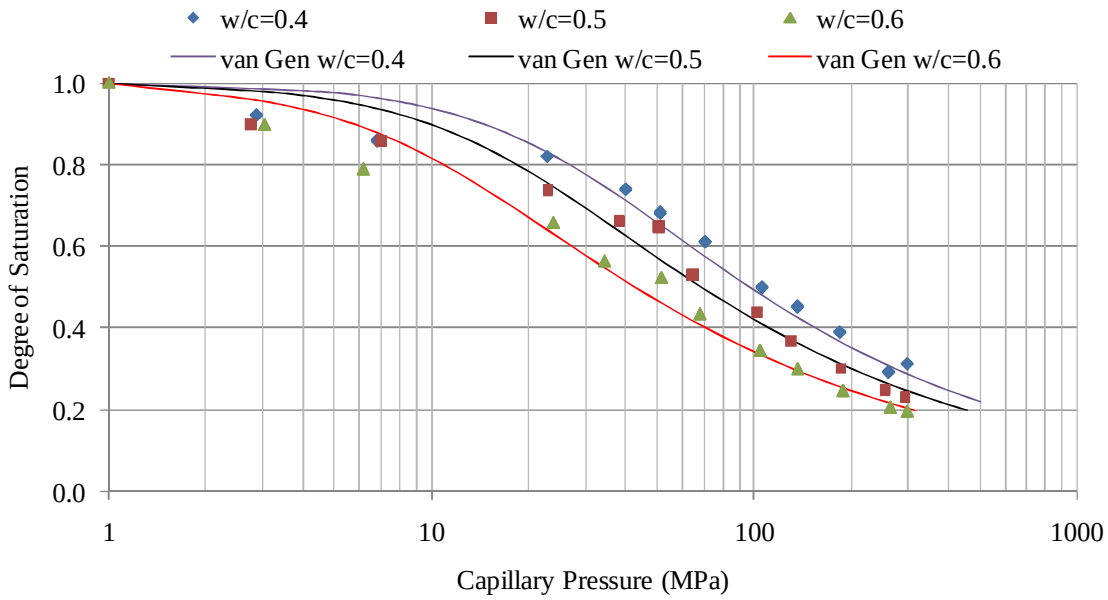

Figure 4-5: Moisture retention curve.

Figure 4-6 shows the liquid (water) relative permeability-saturation relationship of the three concrete mixes using van Genuchten-Mualem model (Mualem 1976; van Genuchten 1980), defined by equation [2-17]. The van Genuchten parameters were used to determine the relative permeability-saturation relationship over the saturation range of 0.2-1.0. The results in Fig. 4-6 showed that the relative permeability strongly depended on the degree of saturation. The form of the curve showed that relative permeability decreased very rapidly with the degree of saturation. The relationship was characterized at higher degrees of saturation by a linear decrease in relative permeability as the degree of saturation decreased, followed by a steep non-linear decrease at lower degrees of saturation. It is evident from Fig. 4-6 that the relative permeability decreased by two-fold when the degree of saturation decreased to 0.7. Similarly shaped profiles were obtained for all the three concrete mixes.

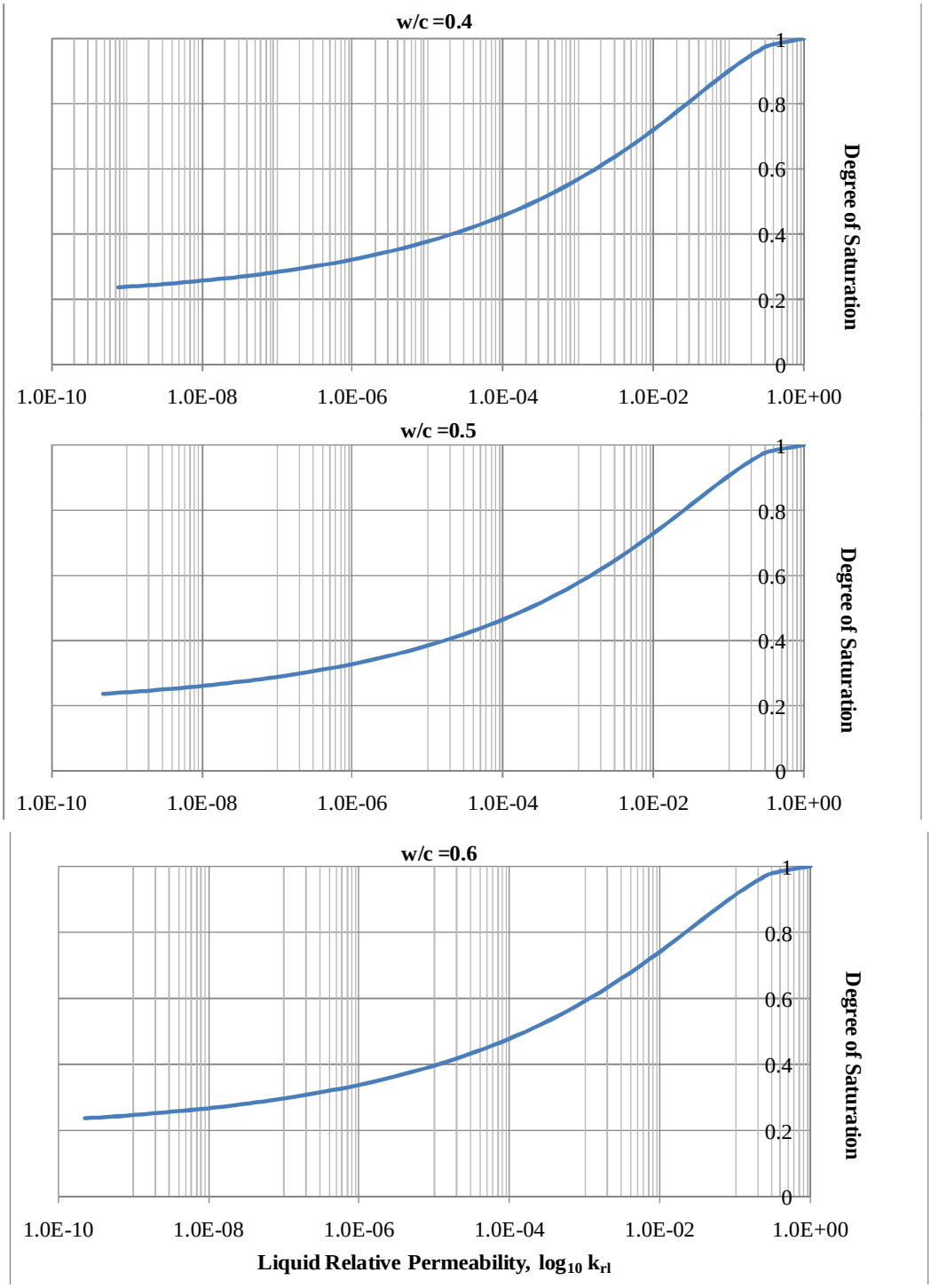

Figure 4-6: Liquid relative permeability curves for concrete (a) w/c = 0.4, (b) w/c = 0.5 and (c) w/c = 0.6.

4.3 Resistivity Test

The dependence of the effective diffusion coefficient on the degree of water saturation of three concrete mixes was obtained using an indirect method of resistivity measurements. The experimental results were compared with other porous materials such as soil and sand. In addition, the suitability of Millington and Quirk model (Millington and Quirk 1961) was validated for concrete.

4.3.1 Saturation Dependence of Chlorides Diffusion

The degree of saturation versus electrical resistivity profiles for different concrete mixes is shown in Figure 4-7. The water saturation of the specimens tested varied from 0.15 to nearly 1.0. The results showed that the electrical resistivity of concrete strongly depended on the degree of saturation and type of concrete. The relationship was characterized at higher degrees of saturation by a gradual increase in electrical resistivity as the degree of saturation decreased, followed by a steep increase at lower degrees of saturation. The steep increase in electrical resistivity at lower degrees of saturation is believed to be due to the reduced ionic mobility as a result of loss of a continuous water phase. Similarly shaped profiles were obtained for all the concrete mixes.

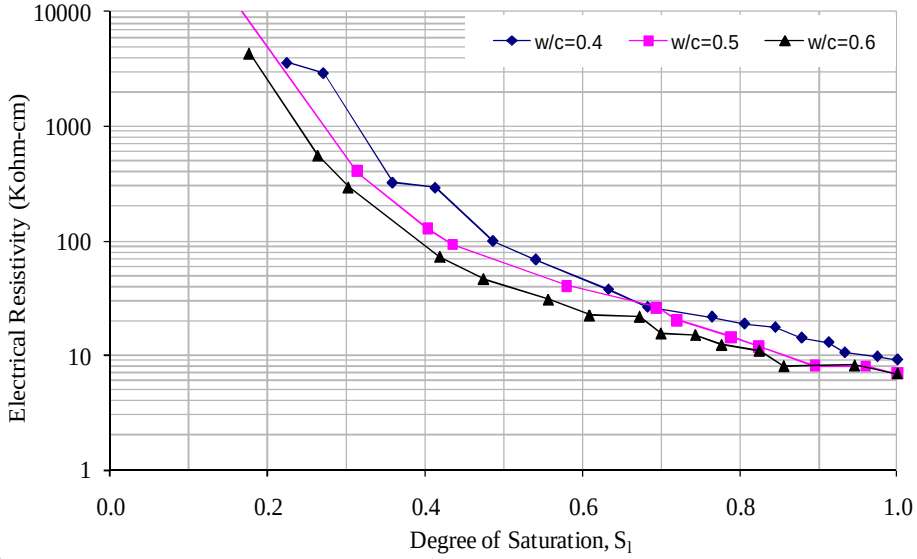

Figure 4-7: Electrical resistivity of concrete at different degrees of saturation.

The results also showed that at a given degree of water saturation, the concrete mix with a lower water/cement ratio had a higher electrical resistivity. This could be attributed to

the decreased connectivity and larger tortuosity of the pore network with decreasing water/cement ratio (Bachmat et al. 1986, McCarter et al. 2001).

To reflect the effect of degree of saturation on the electrical resistivity, the measured electrical resistivity data, shown in Figure 4-7, was converted to normalized resistivity (N_ρ) with respect to the electrical resistivity at full saturation:

$$N_\rho = \frac{\rho}{\rho_s} \qquad [4\text{-}1]$$

where ρ_s is the electrical resistivity measured when the degree of saturation was equal to 1.0, and ρ is the electrical resistivity measured at any other saturation. The normalized resistivity values were used to determine the relative changes in resistivity with changing levels of saturation. The effect of the degree of saturation on the electrical resistivity is shown in Figure 4-8 for different concrete mixes. The results in Figure 4-8 show that the normalized resistivity increases with a decrease in the degree of saturation.

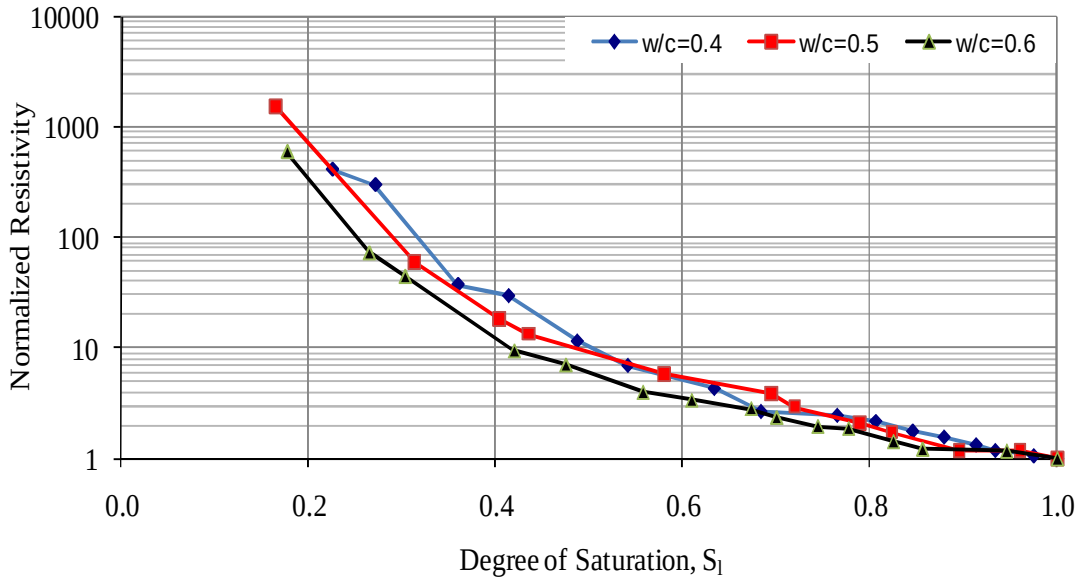

Figure 4-8: Normalised resistivity of concrete.

As discussed in Section 2.2.3(b), the electrical conductivity of a porous medium and the effective diffusion coefficient are directly related to each other. Martys (1999) and

Polder et al. (2002) used electrical conductivity measurements in concrete to calculate the relative diffusion coefficient; the results were in good agreement with experimental results. Diffusion coefficients calculated from electrical conductivity measurements have been compared with self-diffusion coefficients obtained by transient state methods in soils and gravels (Conca and Wright 1990).

The normalized electrical resistivities, shown in Figure 4-8, were converted to normalized electrical conductivities using equation [2-37]. The effect of the degree of water saturation on normalized electrical conductivity and, analogously, on the relative diffusion coefficient, D_{eff} (S_l < 1.0) / D_{eff} (S_l = 1.0), is shown in Figure 4-9 for three different concrete mixes. The results in Fig. 4-9 showed that the relative diffusion coefficient decreased with decreases in the degree of saturation. The decrease was quite rapid initially for all the three concrete mixes, especially for a w/c ratio of 0.4. However, below a degree of saturation of about 0.7, the decrease was less rapid. There was a significant decrease in relative diffusion coefficient at, or around, a degree of saturation of about 0.6. The relative diffusion coefficient was about 0.2 for the concrete mix with w/c ratios of 0.4 and 0.5 and slightly higher for the concrete mix with a w/c ratio of 0.6 at a degree of saturation of about 0.6. It was found that the relative diffusion coefficient decreased much more quickly than the degree of saturation, and goes to zero at, or around, a degree of saturation of about 0.2. This could be possibly due to the development of a discontinuous liquid phase at, and below, a degree of saturation of around 0.2. Figure 4-10 shows that, for the concrete mix with a w/c ratio of 0.6, the value of the relative diffusion coefficient at any given degree of saturation was much higher than those for w/c ratios of 0.4 and 0.5. In general, the relative diffusion coefficient decreased with a decrease in the degree of saturation. Also, the form of the functional relationship between the relative diffusion coefficient and the degree of saturation was non-linear for all the concrete mixes.

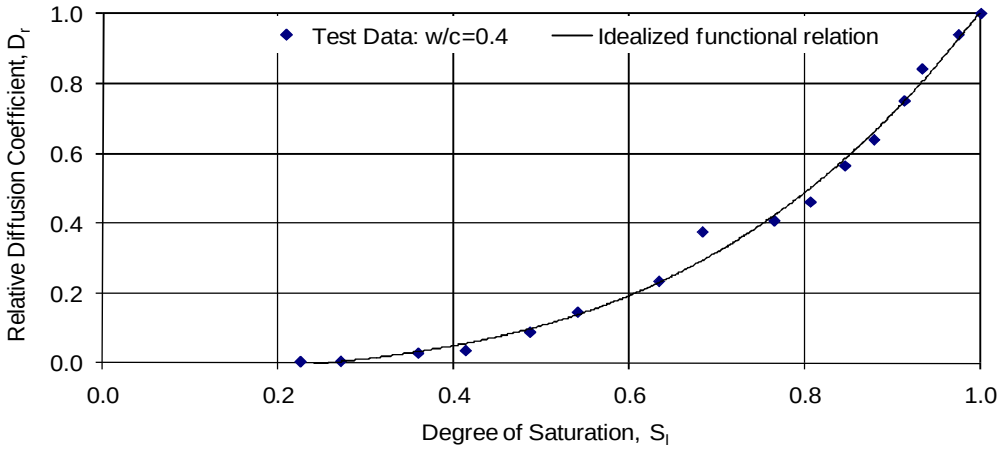

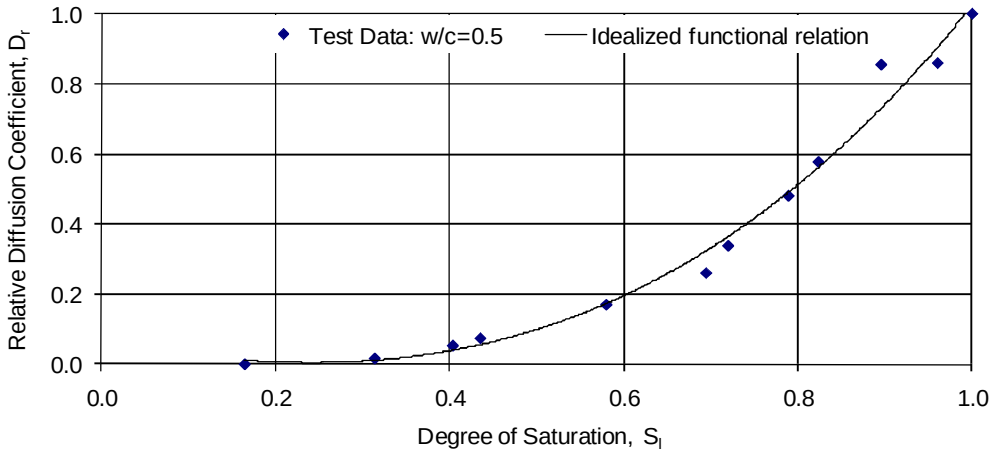

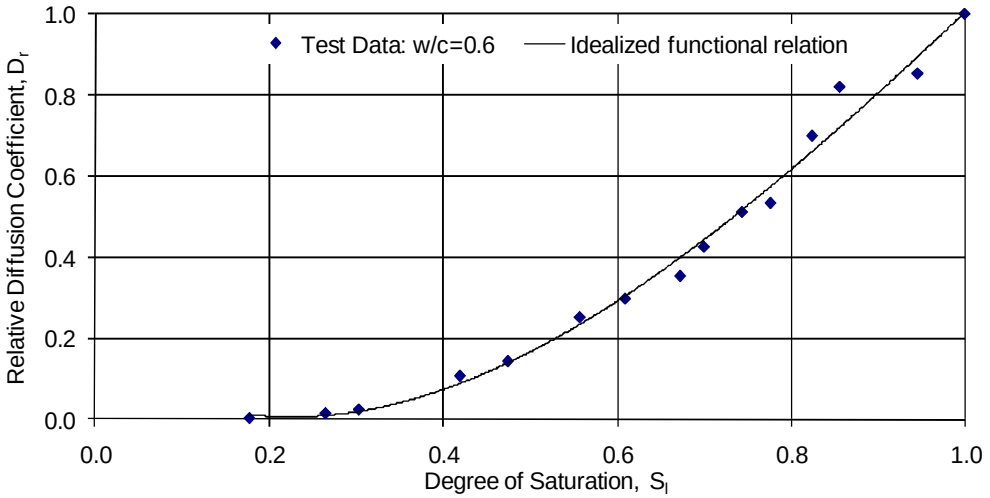

Figure 4-9: Relative diffusion coefficient curves for concrete: (a) w/c ratio=0.4, (b) w/c ratio=0.5, and (c) w/c ratio=0.6.

The relationship between the degree of saturation and the relative diffusion coefficient for concrete is compared with experimental data for sand from Barbour et al. (1996) and Lim et al. (1998), as shown in Figure 4-10. Although, the form of the functional relationship between the degree of saturation and the relative diffusion coefficient for sand showed a decrease in the relative diffusion coefficient with a decrease in degree of saturation similar to that of concrete, the functional relationship was not as non-linear as that of concrete.

The results in Figure 4-10 showed that, with an increased w/c ratio, the non-linearity of the functional relationship between the degree of saturation and the relative diffusion coefficient decreased. This could possibly be attributed to the increased porosity associated with the increased water-cement ratio, and is consistent with the fact that sand, having a larger porosity in comparison to concrete showed much less non-linearity.

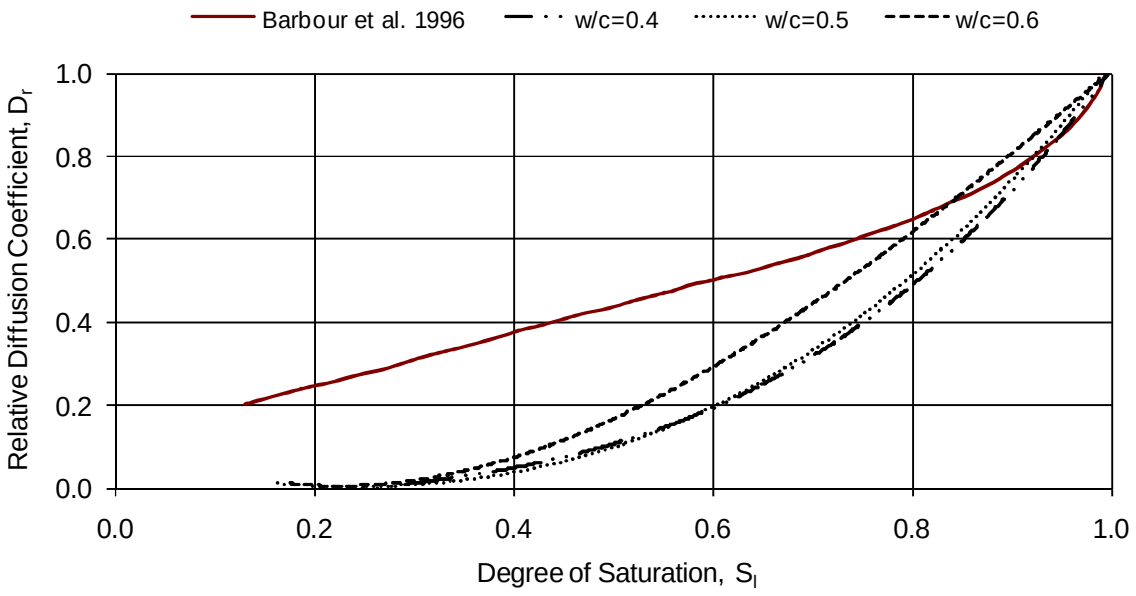

Figure 4-10: Comparison between the relative diffusion coefficient curves for concrete and sand.

The effect of degree of saturation on the relative diffusion coefficient of concrete was found to be adequately representable with the Millington and Quirk (1961) model (MQ).

To compare the effect of degree of saturation on the relative diffusion coefficient with MQ model, the model needs to be normalized with respect to the porosity term. The saturation dependent tortuosity of the normalized MQ model is given by:

$$\tau(s_l) = \frac{\beta}{\varphi^{4/3}} = S_l^{10/3} \qquad [4\text{-}2]$$

where $\tau(s_l)$ is the saturation dependent tortuosity.

A comparison between the normalized MQ model and the experimental degree of saturation versus relative diffusion coefficient data is shown in Figure 4-11. The results in Figure 4-11 showed that similarly shaped profiles were obtained using both experimental data and the normalized MQ model. The results in Figure 4-11 clearly showed that the experimental relative diffusion coefficient values were in very good agreement with normalized MQ model for concrete mixes with w/c ratios of 0.4 and 0.5. For a water cement ratio of 0.6, however the experimental values were nearly 15% higher than those calculated using the normalized Millington-Quirk model. Table 4-3 shows a comparison between the test results and the Millington and Quirk model.

Table 4-3: Relative difference between test data and Millington and Quirk model

	w/c-0.4	w/c-0.5	w/c-0.6
Correlation coefficient (R^2)	0.99	0.97	0.96
Root mean-squared error (%)	3.41	6.86	9.71
Mean absolute error (%)	2.42	4.27	6.92
Relative absolute error (%)	7.51	15.03	23.70

The experimental results show that the Millington and Quirk model, which was originally developed for soils, is also applicable to concrete.

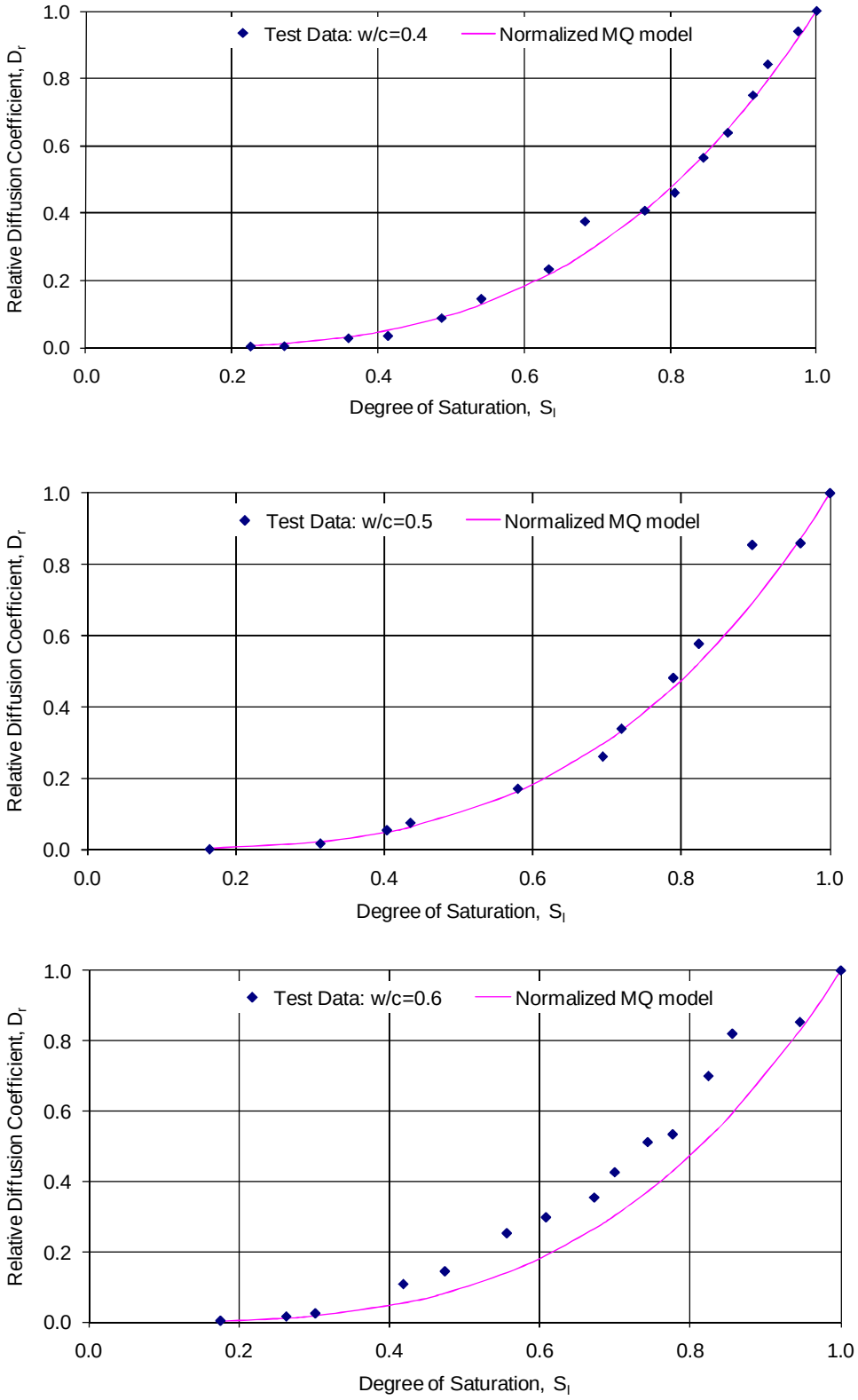

Figure 4-11: Comparison between test result and Normalized MQ model.

4.4 Numerical Modelling

The experimental results discussed earlier were used as input parameters in a computer simulator, TOUGH2, to determine their influences on water flow and transport of chlorides in unsaturated concrete. TOUGH2 (Pruess et al. 1999), is a multicomponent, multiphase simulator of water dynamics in porous media. It has been extensively validated on a series of unsaturated flow problems (Moridis and Pruess 1992; Pruess et al. 1996). It solves mass and energy balance equations (see Section 2.1.2) that describe fluid flow and heat transfer in general multiphase, multicomponent systems. Fluid advection is described with a multiphase extension of Darcy's law; in addition there is diffusive mass transport in all phases. It is capable of modelling both isothermal and non-isothermal conditions. It uses a variety of different functions to model relative permeability and capillary pressure, including the functions of van Genuchten (van Genuchten 1980) and Mualem (Mualem 1976), among others. The EWASG module of TOUGH2 was used to run the simulations. The EWASG (Water-Salt-Gas) module models two phase salt dynamics, along with unsaturated flow. EWASG represents the active system components (water, NaCl, air) as two-phase (liquid and gas) mixtures. A detailed description of EWASG is outside the scope of this work.

Influence of various parameters on ionic transport

The numerical solutions were carried out on a 200 mm thick concrete specimen, modeled as a one grid block wide column with cross-sectional area of $1cm^2$. The problem simulates one-dimensional flow with constant surface chloride concentration. The concrete was discretized by using one 1mm, one 2mm, one 3mm, one 4 mm, and thirty eight 5mm rectangular elements, respectively. The smaller elements were used at the boundary to accurately capture the transient conditions at the boundary. The numerical solutions obtained for other mesh sizes (up to 15 mm) were also identical in the case of wetting phase. The geometry, mesh and boundary conditions used are shown in Figure 4-12. The concrete was subjected to constant chloride concentrationalong the right-hand boundary to simulate an atmospheric boundary. The atmospheric boundary was modelled as a 0.1 mm thick element with a volume factor of 1E+50 to make the boundary volume infinite. The atmospheric boundary element was modeled as an

"inactive" element in order to maintain its properties as constant throughout the simulations. In TOUGH2, constant Dirichlet (essential) boundary conditions are set by using an "inactive" grid block (i.e. grid block which gets involved in flow equations but whose initial conditions remain constant). The top, bottom and left-hand boundaries of concrete were modeled as no flow boundaries, to simulate the concrete edge.

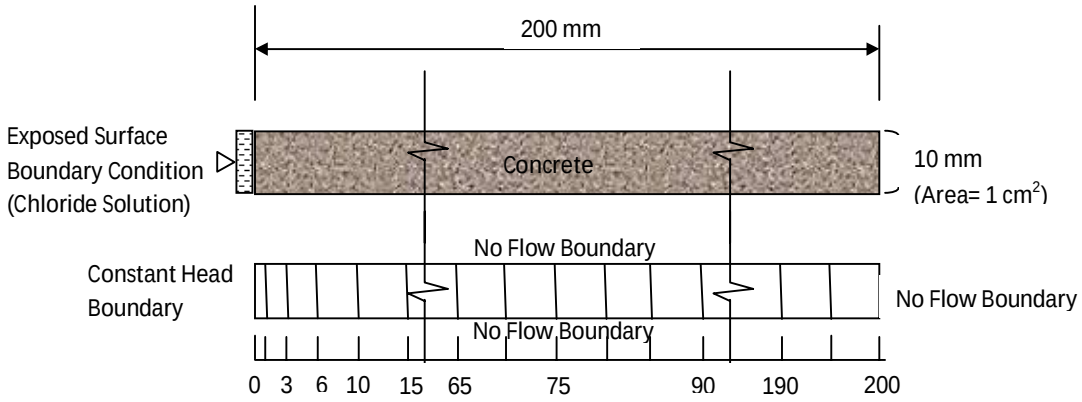

Figure 4-12: Geometry, mesh and boundary conditions used for all numerical analysis

The input parameters to the simulations were evaluated from experimental results and shown in Table 4-4. The initial chloride concentration inside the concrete was set at zero for all the analyses. The temperature was kept constant during the analysis at 22 °C since all the experiments were carried out at this temperature. The diffusion coefficient and surface chloride concentration values were chosen arbitrarily for the purpose of these simulations. The initial conditions and boundary conditions used for the simulations are shown in Table 4-4. All the simulation results reported here were made for concrete during its wetting phase.

The drying phase results are not reported here due to the large amount of chloride loss during the drying phase. The chloride loss could be attributed to the very strong capillary pressure that develops inside a drying concrete. In reality, chloride binding plays a major role in the stability of the solution under evaporative boundary conditions and cannot be ignored or accounted for, indirectly, through a lower diffusion coefficient. TOUGH2

does not have a provision to implement chloride binding. Therefore, chloride concentration profiles during the drying phase were not in good agreement with those present in the literature. There is a need for further study to resolve the issue of chloride loss during the drying phase simulation using TOUGH2.

The influence of the experimental parameters, measured above, on chloride ingress was studied by analyzing three different cases: one in which the initial saturation of a given concrete mix (w/c=0.4) was varied ($0.5 \leq S_l \leq 1.0$) (diffusion and convection); a second one in which for a given initial saturation ($S_l=0.8$) the concrete mix properties were varied (diffusion and convection); and, a third one in which the initial saturation of a given concrete mix (w/c=0.4) was varied ($0.2 \leq S_l \leq 1.0$) (only diffusion). The concrete was subjected to a constant chloride concentration at the boundary in all the three cases.

Table 4-4: Parameters used for simulation in TOUGH2

Concrete Properties				
Mix Type		w/c=0.4	w/c=0.5	w/c=0.6
Density (kg/m^3)		2420	2390	2340
Porosity		0.115	0.121	0.131
Saturated Permeability (m^2)		9.10 E-19	2.16E-18	6.01 E-18
Diffusion Coefficient for saturated concrete (m^{2}s^{-1})		2.087E-10	2.087E-10	2.087E-10
Relative Permeability (van Genuchten-Mualem model) Parameters	RP(1)	0.3455	0.3371	0.3248
	RP(2)	0.1	0.1	0.1
	RP(3)	1.0	1.0	1.0
	RP(4)	0.01	0.01	0.01
Capillary Pressure(van Genuchten function) Parameters	CP(1)	0.3455	0.3371	0.3248
	CP(2)	0.1	0.1	0.1
	CP(3) (1/Pa)	3.494E-08	5.174E-08	9.04E-08
	CP(4) (Pa)	1.0E10	1.0E10	1.0E10
	CP(5)	1.0	1.0	1.0

Initial Condition(Concrete)				
Phase	Pressure(Pa)	Temperature (°C)	Liquid saturation	Salt Mass Fraction
Two Fluid Phase	1.013E+05	22	varies	0
Boundary Condition-Wetting Phase				
Single Fluid Phase (Fixed State)	1.013E+05	22	1	XNaCl =0.05 (=50 kg/m^3 of pore solution)

The results of the numerical analyses are presented in the following sections.

4.4.1 Influence of degree of saturation on chloride penetration

The effect of the degree of saturation on chloride penetration was studied by running an example where the initial degree of saturation of a given concrete mix (w/c=0.4) was varied ($0.5 \leq S_l \leq 1.0$). Input parameters used to run the simulation are listed in Table 4-4. To evaluate the influence of the degree of saturation on chloride penetration, only the initial degree of saturation of concrete was varied while maintaining the other concrete properties, as well as the boundary conditions, was constant. The results of the numerical analysis are shown in Figure 4-13 (a) and 4-13 (b), where chloride concentration profiles after an exposure period of 5 hours and 24 hours are plotted with depth, respectively.

The results show that the initial level of saturation greatly affects the resulting chloride profile. The concrete with initial lower saturation values showed higher chloride concentrations at a given depth compared to a concrete with higher saturation values, even though the same external boundary conditions were applied in all cases. This result can be explained as follows: with a decrease in saturation, capillary pressure increased (see Figure 4-5) which, in turn, increased the liquid flux drawn inside the concrete through advection according to equation [2-16]. The increased liquid flux resulted in more chloride transport. For the same reason, the chloride penetration depth was also higher for the case of lower saturation.

Figure 4-13 (b) shows that there was a large increase in the penetration depth from 5 hours to 24 hours; the chloride concentration was also higher at this time. However, the rate of increase of chloride concentrations reduced; the reduced rate of increase of chloride concentrations is mainly due to the effect of time on the saturation of concrete. With time, the saturation of the concrete increased, as more moisture was drawn inside the concrete. That decreased the capillary pressure and moisture flux. Moisture flow due to capillary pressure contributed to pull the penetration front inward and thus increased the penetration depth. When the saturation of concrete was low, advective transport was the dominant transport mechanism. However, as saturation level increased to near full saturation diffusive transport became a dominant transport mechanism.

(a)

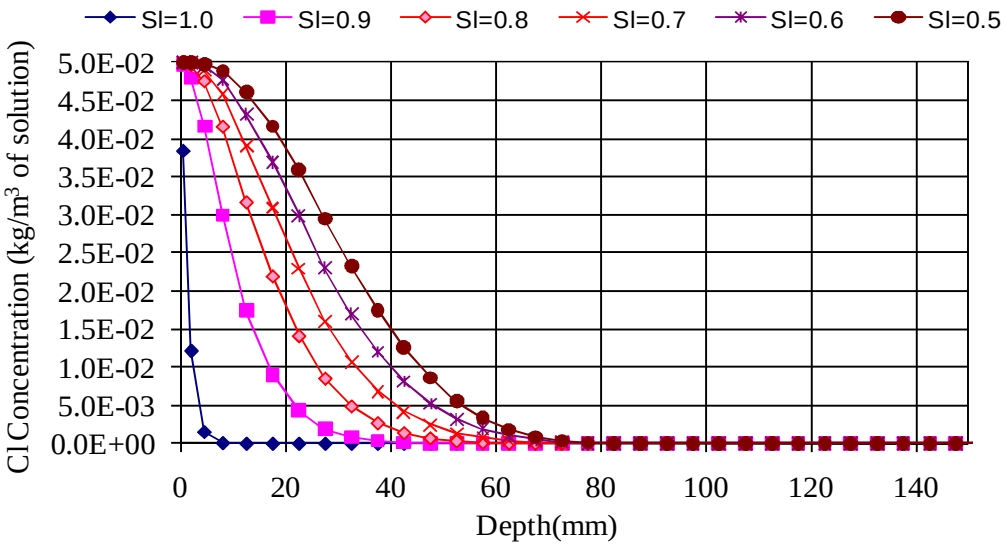

(b)

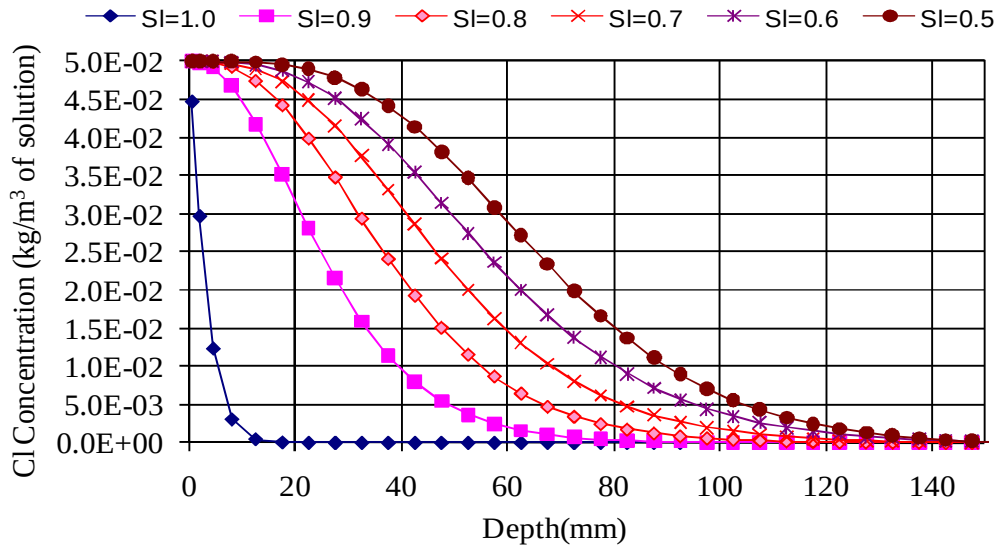

Figure 4-13: Chloride profile in concrete at different degree of saturation for w/c=0.4 (a) after 5 hours of wetting, and (b) after 24 hours of wetting.

It is observed in Figure 4-13 that both the chloride concentration and penetration depths were higher in concrete with saturation values lower than 1.0 (unsaturated concrete) compared to concrete with saturation value 1.0 (fully saturated concrete). This is due to the dominance of combined diffusive and advective transport of chlorides in unsaturated concrete compared to purely diffusive transport in fully saturated concrete, as mentioned

in Section 2.2.2. This result emphasizes the importance of modelling water flow and the transport of chlorides in unsaturated conditions when predicting the service life of a concrete structure.

It is expected that similar results will be obtained for other concrete mixes. This is the reason why the example was run using only one concrete mix.

4.4.2 Influence of concrete mix on chloride penetration

The effect of the concrete mix design on chloride penetration was studied by running an example in which for a given initial saturation (S_l =0.8), the concrete mix properties were varied. Three different concrete mixes, with w/c ratios of 0.4, 0.5 and 0.6 were used for this example. Input parameters used to run the simulation are listed in Table 4-4. The initial saturation of the concrete was chosen arbitrarily. To evaluate the influence of the concrete mix on chloride penetration, only concrete mix properties were varied while maintaining the initial saturation as well as chloride concentration at the boundary constant. The results of the numerical analysis are shown in Figure 4-14 (a) and 4-14 (b), where chloride concentration profiles after an exposure period of 5 hours and 24 hours are plotted with depth, respectively.

The results showed that the w/c ratio of concrete greatly affects the resulting chloride profile. Note that concrete with higher water-cement ratios showed higher chloride concentrations at a given depth compared to the concrete with lower water-cement ratios, even though the same external, constant concentration boundary condition was applied in all cases. This result can be explained as follows: with an increased water-cement ratio, the saturated hydraulic conductivity of the concrete increased (see Figure 4-1; Table 4-1). The increase was so substantial that the liquid flux drawn inside the concrete increased (see equation [2-16]), even though the capillary pressure was lower compared to concrete with lower w/c ratios (see Figure 4-5). The increased liquid flux resulted in more chloride transport. For the same reason, the chloride penetration depth was also higher for the case of higher water-cement ratios.

(a)

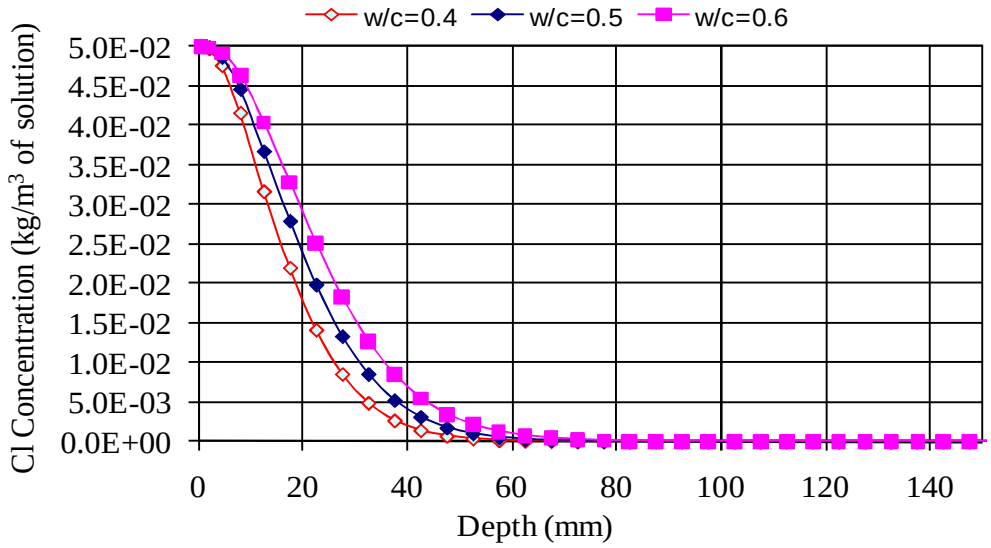

(b)

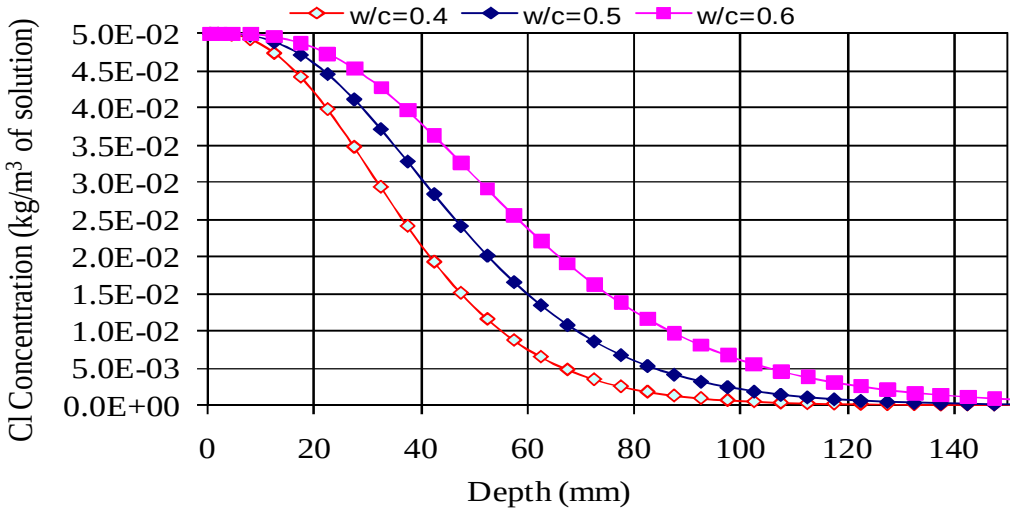

Figure 4-14: Chloride profiles at S_l =0.8 for three different concrete mixes (a) after 5 hours of wetting, and (b) after 24 hours of wetting.

Figure 4-14 (b) showed that there was a large increase in the penetration depth from 5 hours to 24 hours, the chloride concentration was also higher at this time. However, the rate of increase of chloride concentration was lower. The reduced rate of increase of the chloride concentration was mainly due to the effect of time on the saturation of concrete. With time, saturation of the concrete increased, as more moisture was drawn inside the

concrete. That decreased the capillary pressure and moisture flux. Moisture flow due to capillary pressure contributed to pulling the penetration front inward and, thus, increased the penetration depth.

It is expected that similar results will be obtained for other concrete saturations.

4.4.3 Influence of degree of saturation on chloride diffusion

The effect of the degree of saturation on chloride diffusion was studied by running an example where the initial degree of saturation of a given concrete mix (w/c=0.4) was varied ($0.2 \leq S_l \leq 1.0$). Input parameters used to run the simulation are listed in Table 4-4. To evaluate the influence of the degree of saturation on chloride penetration due to diffusion, only the degree of saturation of the concrete was varied while maintaining all the other concrete properties as well as the boundary conditions. The value of the saturated hydraulic permeability of the concrete mix was set at zero to force the chloride transport due to diffusion only. The Millington and Quirk model was used to model the saturation dependence of the diffusion coefficient in the simulator. The results of the numerical analysis are shown in Figure 4-15, where chloride concentration profiles after an exposure period of 10 days are plotted with depth. The exposure period was chosen to be longer compared to the previous examples due to the slow process of diffusion.

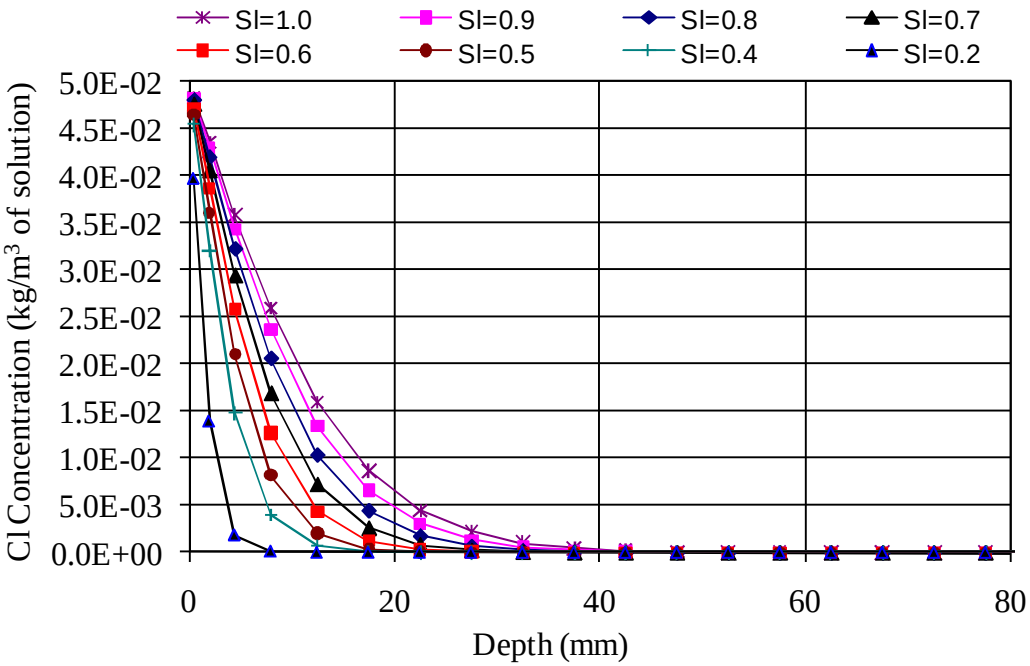

Figure 4-15: Chloride diffusion in concrete at different degree of saturation for w/c=0.4 after 10 days.

The results showed that the saturation of concrete greatly affects the resulting chloride profile. Note that the concrete with higher saturation values showed higher chloride concentrations at a given depth compared to concrete with a lower saturation value, even though the same external boundary conditions were applied to all cases. This was as expected, since, with increased saturation the effective diffusion coefficient increased (see Figure 4-9 and 4-11) which, in turn, increased the diffusive flux inside the concrete, according to equation [2-28]. The increased diffusive flux resulted in more chloride transport. For the same reason, the chloride penetration depth was also higher for the case of higher saturation.

It is expected that similar results would be obtained for other concrete mixes as well with the only difference in the amount and depth of chloride penetration due to different porosity and diffusion coefficient value, if used different values for each mix.

The above simulations suggest that how the transport properties measured in this study affect the ingress of chlorides in unsaturated concrete. They also suggest that multiphase, multicomponent approaches can be used as a powerful tool for predicting the long term performance of concrete under unsaturated conditions.

4.5 Summary

The saturated hydraulic conductivity of three concrete mixes was obtained using a centrifuge technique. Twelve concrete samples were tested, four for each of three w/c ratios. The mean saturated hydraulic conductivity was 9.0E-12 m/s for w/c of 0.4, 3.1E-11 m/s for w/c of 0.5 and 5.9E-11 m/s for w/c of 0.6. The results showed that an increase in water-cement ratio increased the hydraulic conductivity of concrete. An increase in the w/c ratio from 0.4 to 0.6 resulted in an increase in the saturated hydraulic conductivity by almost seven times.

The moisture retention curves of three concrete mixes were determined using the vapour equilibrium technique. The test results showed that the degree of water saturation of the concrete samples decreased with a decrease in relative humidity. For a given relative humidity boundary condition, the degree of saturation was higher for the samples with lower w/c ratios. The results also showed that the capillary pressure increased gradually as the degree of water saturation decreased. Similarly shaped profiles were obtained for all the three concrete mixes. The experimental moisture retention data was used to determine the van Genuchten parameters for each concrete mix type. The van Genuchten parameters provide the means for determining a closed-form relationship between capillary pressure-saturation and relative permeability-saturation over the entire saturation range. The results showed that the relative permeability strongly depended on the degree of saturation. The relationship between saturation and relative permeability was characterized at higher degrees of saturation by a decrease in relative permeability as the degrees of saturation decreased, followed by a steep non-linear decrease at lower degree of saturation. It was found that, for all the three concrete mixes the relative

permeability decreased by a factor of two orders of magnitude when the degree of water saturation decreased from 1.0 to 0.7.

The dependence of the effective diffusion coefficient on the degree of water saturation was determined using a resistivity technique for three different concrete mixes. This experimental result is very valuable, considering the fact that there are very little data available in the literature showing this dependence for concrete. The results showed that the electrical resistivity of concrete strongly depended on the degree of water saturation, as well as the w/c ratio of concrete. The normalized electrical resistivities were converted to relative diffusion coefficients. These results showed that the relative diffusion coefficient decreased with a decrease in the degree of saturation. The decrease was quite rapid initially for all the three concrete mixes, especially for a w/c ratio 0.4. However, below a degree of saturation of about 0.6, the decrease was less rapid. There was a significant decrease in the relative effective diffusion coefficient at, or around, a degree of saturation of about 0.6. In general, the relative diffusion coefficient decreased with a decrease in the degree of saturation. Also, the form of the functional relationship between the relative diffusion coefficient and the degree of saturation was non-linear for all the concrete mixes.

The degree of saturation versus relative diffusion coefficient relationship for concrete was compared with experimental data on sand that was taken from the literature. The form of the functional relationship between the degree of saturation and the relative diffusion coefficient for sand also showed a decrease in the relative diffusion coefficient, with a decrease in degree of saturation similar to that of concrete, although the functional relationship was not as non-linear as that of concrete. A comparison was also made between the normalized form of the Millington and Quirk (MQ) model and the experimental degree of saturation versus relative diffusion coefficient data. The results showed that similarly shaped profiles were obtained using both experimental data and the normalized Millington and Quirk model. The results clearly showed that the experimental relative diffusion coefficient values were in very good agreement with normalized MQ model for concrete mixes with w/c ratios of 0.4 and 0.5. For a water

cement ratio of 0.6, the experimental values were nearly 15% higher than those calculated using the normalized Millington-Quirk model.

Numerical modelling was carried out to investigate the influence of various parameters measured in this study on water flow and the transport of chloride in unsaturated concrete. TOUGH2, a multicomponent, multiphase simulator, was used to run the simulations.

Simulations were run to show the effect of the degree of saturation on chloride penetration using concrete with a w/c of 0.4. Simulations were carried out on concrete with different initial degrees of water saturation. The results showed that the chloride penetration profile strongly depended on the degree of saturation of the concrete. The relationship was characterized by an increasing amount of chloride penetration as the initial degree of water saturation of concrete was decreased.

Simulations were run to reflect the effect of three different concrete mixes, with w/c ratios of 0.4, 0.5 and 0.6, on the depth of chloride penetration at a given degree of water saturation. The results showed that the chloride penetration profile strongly depended on the w/c ratio of the concrete mix. The relationship was characterized by a higher degree of chloride penetration with a higher w/c ratio.

Simulations were also run to reflect the effect of the degree of saturation on the depth of chloride penetration due to a purely diffusive transport. A concrete mix with a w/c ratio of 0.4 was used for this study. The Millington and Quirk model was used for determining the saturation dependence of the diffusion coefficient. The degrees of water saturation of the concrete were varied from 0.2 to 1.0. The results showed that the chloride penetration due to a diffusive transport depended strongly on the degree of water saturation of the concrete. The relationship was characterized by an increased amount of chloride penetration as the initial degree of water saturation of concrete was increased.

5 Conclusions & Recommendations

This chapter provides a summary of the work and conclusions, with reference to the objectives of the research. Recommendations are also provided for future research on this subject matter.

5.1 Summary of work

1. The principles of moisture flow and the transport of chlorides in unsaturated concrete were discussed. The standard experimental methods available in the literature were also discussed in terms of their applicability to the case of unsaturated flow.
2. Three different experiments were performed to determine the saturated hydraulic conductivity, the moisture retention function, and the dependence of the effective diffusion coefficient of concrete on saturation. The experiments were carried out on samples prepared from three different concrete mixes, with w/c ratios of 0.4, 0.5 and 0.6. The physical properties of the concrete mixes were determined experimentally.
3. A centrifugation technique was used to determine the saturated hydraulic conductivity of the three concrete mixes. The experiment was carried out on twelve concrete samples, four from each of three concrete mixes. Using this technique, the saturated hydraulic conductivity measurements were made within 24 hours.
4. A vapour equilibrium technique was used for determining the moisture retention function of concrete. The experiments were carried out on three different concrete mixes at a constant temperature of 22±0.5°C. Twelve different desorption environments were imposed on the concrete specimens by using twelve different saturated salt solutions kept in closed containers. The degree of water saturation of the samples was determined at the end of the experiment. The experimental moisture retention data was used to determine van Genuchten

parameters for each concrete mix type. The van Genuchten parameters provided the means for determining a closed-form relationship between the capillary pressure-saturation and the relative permeability-saturation over the entire saturation range.

5. The resistivity technique was used to characterize the effect of the degree of saturation on the effective diffusion coefficient. DC voltage was used for determining the electrical resistivity of concrete. Three samples were tested from each concrete mix. Two different voltages, 5.0 V and 2.5 V, were applied on each sample at different degrees of water saturation. The degree of water saturation of the samples and currents corresponding to each voltage were measured during the experiment. The degree of saturation versus relative diffusion coefficient relation of the concrete was compared with experimental data on sand that was presented in the literature. A comparison was also made between the normalized form of the Millington and Quirk (MQ) model and the experimental degree of saturation versus relative diffusion coefficient data.
6 .Numerical simulations were carried out to show the influence of various parameters measured in this study on water flow and the transport of chlorides in unsaturated concrete. TOUGH2, a multicomponent, multiphase simulator was used to perform the simulations.

5.2 Important findings

1. The mean value of saturated hydraulic conductivity was 9.0E-12 m/s for w/c of 0.4, 3.1 E-11 m/s for w/c of 0.5 and 5.9E-11 m/s for w/c of 0.6. The results showed that an increase in water-cement ratio increased the hydraulic conductivity of concrete. An increase in the w/c ratio from 0.4 to 0.6 increased the saturated hydraulic conductivity by almost seven times. The largest coefficient of variation in the measured saturated hydraulic conductivity was 11.1 %, which confirms that the centrifugal technique has the potential for yielding reliable estimates of the saturated hydraulic conductivity in a very short period of time as compared to other standard methods.

2. The test results showed that the degree of water saturation of the concrete samples decreased with a decrease in relative humidity. For any particular relative humidity boundary condition, the degree of saturation was higher for the samples with lower w/c ratios. The results also showed that capillary pressure increased gradually as the degree of water saturation decreased. Similarly shaped profiles were obtained for all the three concrete mixes. The results showed that the relative permeability strongly depended on the degree of saturation. The relationship between saturation and relative permeability was characterized at higher degrees of saturation by a linear decrease in relative permeability as the degree of saturation decreased, followed by a steep non-linear decrease at lower degree of saturation. It is found that, for all the concrete mixes, the relative permeability decreased by a factor of two orderswhen the degree of water saturation decreased from 0.1 to 0.7.
3. The results showed that the relative diffusion coefficient decreased with decreasing degrees of saturation. The decrease was initially quite rapid for all the three concrete mixes, especially for a w/c ratio of 0.4. However, below a degree of saturation of about 0.6, the decrease was less rapid. There was a significant decrease in the relative effective diffusion coefficient at, or around, a degree of saturation of about 0.6. In general, the relative diffusion coefficient decreased with a decrease in the degree of saturation. Also, the form of the functional relationship between the relative diffusion coefficient and the degree of saturation was non-linear for all the concrete mixes tested. When compared with Millington and Quirk(MQ) model, the results showed that similarly shaped profiles were obtained using both experimental data and the normalized Millington and Quirk model. The results clearly showed that the experimental relative diffusion coefficient values were in very good agreement with normalized MQ model for concrete mixes with w/c ratios of 0.4 and 0.5. For a water cement ratio of 0.6, the experimental values were nearly 15% higher than those calculated using the normalized Millington-Quirk model. The above experimental results are very valuable, considering the fact that there are very little data available in the literature showing this dependence in the case of concrete.
4. The simulation results showed that the chloride penetration profile strongly depended on the degree of saturation of the concrete. The relationship was

characterized by an increasing amount of chloride penetration as the initial degree of water saturation of the concrete decreased.

5. The simulation results showed that the chloride penetration profile strongly depended on the w/c ratio of the concrete. The relationship was characterized by a higher amount of chloride penetration with higher w/c ratios of the concrete.
6. The simulation results showed that the chloride penetration due to diffusive transport depended strongly on the degree of water saturation of the concrete. The relationship was characterized by an increased amount of chloride penetration as degree of water saturation of the concrete increased. When the degree of water saturation decreased to 0.2, the chloride diffusion into the concrete decreased to almost zero.

5.3 Conclusions

1. A sound theoretical framework has been proposed for modeling water flow and transport of chlorides in concrete under unsaturated condition.
2. Novel experimental techniques, initially developed in other areas such as soil sciences and petroleum engineering, have been used and shown to work very nicely for concrete.
3. Using the experimental data generated in this study, numerical simulations have been carried out to investigate the effect of each parameter on the movement of moisture and the transport of chlorides in unsaturated concrete.

5.4 Recommendations for future work

1. The experimental program could be extended by varying more parameters than simply the w/c ratio (for example, the cement type, mineral additions, admixtures, etc.) and studying their effects on the transport properties of concrete.

2. It is believed that improved performance predictions of concrete structures would be achieved by integrating direct modelling of chloride binding and corrosion into the current model. This would lead to a more realistic prediction of time to cracking of reinforced concrete structures and, hence, allowing the implementation of effective maintenance strategies for our aging infrastructure.

3. The ”salt transport” doesn’t “work quite well” for drying phase using TOUGH2. There is a need for further study to resolve this issue.

6 References

Alemi, M.H., Nielsen, D.R., and Biggar, J.W., 1976, Determining the Hydraulic Conductivity of Soil Cores by Centrifugation, *Soil Science Society American Journal*, Vol. 40.

Andrade, C., Alonso, C., and Goni, S., 1993, Possibilities for Electrical Resistivity to Universally Characterise Mass Transport Process in Concrete, *Proceedings of the Concrete 2000 Conference*, Vol. **2**., R. K. Dhir and M. R. Jones, Eds. E & FN Spon, London, pp. 1639-1652

Arulanandan, K., 1988, Centrifuge Modelling of Transport Processes for Pollutants in Soils, *Journal of Geotechnical Engineering*, Vol. 114, No. 2.

Atkinson, A., and Nickerson, A.K., 1984, The diffusion of ions through water-saturated cement, *Journal of Materials Sciences*, Vol. 19, pp. 3068-3078.

Babaei, K. and Hawkins, N.M. 1988. Evaluation of Bridge Deck Protective Strategies. *Concrete International,* American Concrete Institute, v.10, No.12, pp. 56-66

Bachmat, Y., and Bear, J., 1986, Macroscopic modelling of transport phenomena in porous media, Vol. 1, pp. 213-240.

Bailey, J. E. and Hampsen, C. J. 1982. The Chemistry of the Aqueous Phase of Portland Cement. *Cement and Concrete Research*, Vol. 12, pp. 227-236

Baroghel-Bouny, V., Mainguy, M., Lassabatere, T., and Coussy, O., 1999, Characterization and identification of equilibrium and transfer moisture properties for ordinary and high-performance cementitious materials, *Cement and Concrete Research*, Vol. 29, pp. 1225-1238.

Basheer, Muhammed P. A., 2001. Permeation Analysis, Handbook of Analytical Techniques in Concrete Science and Technology, edited by Ramachandran, V.S.; Beaudoin, J.J., William Andrew Publishing/Noyes. pp. 658-737.

Battistelli, A., Calore, C., and Pruess, K., 1997, The Simulator TOUGH2/EWASG for modelling geothermal reservoirs with brines and non-condensible gas, *Geothermics*, Vol. 26, No. 4, pp. 437-464

Barbour, S. L., Lim, P. C., and Fredlund, D. G. 1996. A New Technique for Diffusion Testing of Unsaturated Soil, *Geotechnical Testing Journal*, GTJODJ, Vol. 19, No. 3, pp. 247-258.

Bazant, Z.P., and Najjar, L.J., 1972, Nonlinear Water Diffusion in Nonsaturated Concrete, *Materials and Strustures (Rilem, Paris)*, Vol. 5, Issue 1, pp. 3-20.

Bear, J., Dynamics of fluids in porous Media, Elsevier, 1972

Bear, J., and Bachmat, Y., 1990, Introduction to Modelling of Transport Phenomena in Porous Media, *Kluwer Academic Publishers*, Dordrecht.

Brakel, J. van, and Heertjes, P.M., 1974, Analysis of diffusion in macroporous media in terms of a porosity, a tortuosity and a constructivity factor, Int. J. *Heat and Mass Transfer*, Vol. 17, pp. 1092-1103.

Brooks, R.H., and Corey, A.T., 1966, Properties of porous media affecting fluid flow, *Proc. Amer. Soc. Civil Eng.*, 92, 61–87.

Carcasses, M., Abbas, A., Olliver, J.P., and Verdier, J., 2002, An optimised pre-conditioning procedure for gas permeability measurement, *Material and Structures*, Vol. 35, pp. 22-27.

Cargill, K.W., and Ko Hon-Yim, 1983, Centrifuge Modelling of Transient Water Flow, *Journal of Geotechnical Engineering*, Vol. 109, No. 4.

Conca, J. L. and Wright, J., 1990, Diffusion Coefficients in Gravel under Unsaturated Conditions, *Water Resource Research*, Vol. 26, No. 5, pp. 1055-1066

Crank, J., 1975, The Mathematics of Diffusion, 2nd ed., Oxford University Press, London, pp. 414.

Dhir, R. K., et al., 1989, Near-Surface Characteristics of Concrete: Prediction of Carbonation Resistance, *Magazine of Concrete Research*, 41(148), 137-143.

Dullien, F.A.L., 1992, Porous Media: Fluid Transport and Pore Structures, *Second edition, Academic Press, Inc.*

El-Dieb, A.S., and Hooten, R.D., 1994, A High Pressure Triaxial Cell with improved measurement sensitivity for saturated water permeability of high performance concrete, *Cement and Concrete Research*, Vol. 24, No. 5, pp. 854-862

European Standard, 1996, Building materials-Determination of hygroscopic sorption curves, ISO/DIS 1257:1996.

Garboczi, E.J., 1990, Permeability, Diffusivity, and Microstructural Parameters: A Critical Review, *Cement and Concrete Research*, Vol. 20, pp. 591-601.

Gardner, W.R., 1958, Some steady state solutions of the unsaturated moisture flow equation, with application to evaporation from a water table, *Soil Sci*., **85**, 228–232.

Goodings, D.J. 1985, Relationships for modelling water effects in geotechnical centrifuge models. *In* Application of centrifuge modelling to geotechnical design, *Edited by* W.H. Craig, A.A. Balkema. Rotterdam, The Netherlands. Pp. 1-24.

Hall, C.,1989, Water sorptivity of mortars and concretes: a review, *Magazine of Concrete Research*, 41, 51-61.

Hall, C., 1994, Barrier performance of concrete: A review of fluid transport theory, *Materials and Structures*, 27, 291-306.

Hall, C., and Hoff, W.D., 2002, Water in porous materials, *Water Transport in Brick, Stone and Concrete*, Spon press, pp. 52-53.

Hansson, I.L.H., and Hansson, C.M., 1983, Electrical Resistivity Measurements of Portland Cement based Materials, *Cement and Concrete Research*, Vol. 13, pp. 675-683.

Homand, F. et al. 2004. Permeability determination of a deep argillite in saturated and partially saturated conditions, In. Jr. of Heat and Mass Transfer, vol. 47, pp. 3517-3531

Kelham, S., 1988, A water absorption test for concrete, *Magazine for Concrete Research*, 40, 106-110.

Khaleel, R., J.F. Relyea, and J.L. Conca. 1995. Evaluation of van Genuchten-Mualem relationships to estimate unsaturated hydraulic conductivity at low water contents. *Wat. Resour. Res*., Vol. 31(11), pp. 2659-2668.

Khanzode, R. M, Vanapalli, S.K, and Fredlund, D.G., 2002, Measurement of soil-water characteristic curves for fine-grained soils using a small-scale centrifuge, *Canadian Geotech. J*., 39**,** 1209-1217.

Labuza T., 1963. Creation of Moisture Sorption Isotherms for Hygroscopic materials. Sorption Isotherm Methods. *International Symposium on Humidity and Moisture*. (www.fsci.umn.edu/Ted Labuza/PDF files/papersCreation Moisture Isotherms.PDF)

Richards, Lorenzo A. 1931. Capillary conduction of liquids through porous mediums, *Physics*, 1, 318-333

Lenhard, R. J. and Parker, J. C. 1987. A model for hysteretic constitutive relations governing multiphase flow, 2. Permeability-saturation relations. *Wat. Resour. Res*., Vol. 23(12), pp. 2197-2206.

Lim, P. C., Barbour, S. L., and Fredlund, D. G. 1998. The influence of degree of saturation on the coefficient of aqueous diffusion. *Can. Geotech. J.*, Vol. 35, pp. 811-827.

Ludirdja, D., Berger, R. L., and Young, J. F., 1989, Simple method for measuring water permeability of concrete, *ACI Material Journal*, Vol. 86, pp. 433-439

McCarter, W.J., 1996, Monitoring the influence of water and ionic ingress on cover-zone concrete subjected to repeated absorption, *Cement Concrete and Aggregate*, ASTM, 18(1), pp. 55-63.

Mainguy, M., Coussy, O., and Baroghel-Bouny, V., 2001. Role of Air Pressure in Drying of Weakly Permeable Materials, *Journal of Engineering Mechanics*, Vol. 127, No. 6, pp. 582-592.

Martys, N.S., 1995, Survey of Concrete Transport Properties and Their Measurement, NISTIR 5592, U.S. Department of Commerce, National Institute of Standards and Technology, Gaithersburg.

Martys, N.S., and Ferraris, C.F., 1997, Capillary Transport in Mortars and Concrete, *Cement and Concrete Research*, Vol. **27**, No.5, pp. 747-760.

Martys, N.S., 1999, Diffusion in partially-saturated porous material, *Materials and Structures*, Vol. 32, October 1999, pp. 555-562.

McCarter, W.J., Chrisp, T.M., Butler, A., and Basheer, P.A.M, 2001, Near-surface sensors for conduction monitoring of cover-zone concrete, *Construction and Building Materials*, 15, pp. 115-124.

Meyer, P.D., Saripalli, K. P. and Freedman, V. L., 2004. Near- Field Hydrology Data Package for the Integrated Disposal Facility 2005 Performance Assessment. PNNL-14700, Pacific Northwest National laboratory, Richland, Washington

Millington, R.J., 1959, Gas diffusion in porous media, *Science*, Vol. 130, pp. 100-102.

Millington, R.J. and Quirk, J.P., 1961, Permeability of Porous Solids, *Transactions of the Faraday Society*, 57, 1200-1207.

Mitchell, R.J. 1991, Centrifuge modelling as a consulting tool, *Canadian Geotechnical Journal*, 28: 162-167.

Mitchell, R.J., 1994, Matrix suction and diffusive transport in centrifuge models, *Canadian Geotechnical Journal*, 31, 357-363.

Monlouis-Bonnaire, J.P., Verdier. J., and Perrin, B., 2004, Prediction of the relative permeability to gas flow of cement-based material, *Cement and Concrete Research*, Vol. 34, pp. 737-744.

Monofore, G.E., 1968, The Electrical Resistivity of Concrete, *Journal of The PCA Research and Development Laboratories*, pp. 35-48.

Mualem, Y., 1976, A new model for predicting the hydraulic conductivity of unsaturated porous media. *Water Resour. Res.,* 12, 513-522**.**

Mualem, Y., 1976, Hysteresis models for prediction of the hydraulic conductivity of unsaturated porous media, *Water Resour. Res.*, 12(6), 1248–1254.

Nilsson, L.O., 1993, Penetration of chlorides into concrete structures – an introduction and some definitions, *Chloride Penetration Into Concrete Structures*, pp. 7-17.

Nilsson, L.O., Poulsen, E., Sandberg, P., Sorensen, H.E., and Klinghoffer, O., 1996, HETEK- Chloride penetration into concrete, State-of-the Art, Transport Processes, Corrosion initiation, Test Methods and Prediction Models, Report No. 53, The Road Directorate, Copenhagen.

Nyame, B. K., 1985. Permeability of Normal and Lightweight Mortars, *Magazine of Concrete Research*, Vol. 37 (130), pp. 44-48.

Nyame, B. K., and Illston, J. M., 1981, Relationship between Permeability and Pore Structures of Hardened Cement Paste, *Magazine of Concrete Research*, Vol.33(116), pp. 139-146.

Parker, J. C. and Lenhard, R. J. 1987. A model for hysteretic constitutive relations governing multiphase flow, 1. Saturation-pressure relations. *Wat. Resour. Res*., Vol. 23(12), pp. 2187-2196.

Polder, R. B., and Peelen, W. H. A., 2002. Characterisation of chloride transport and reinforcement corrosion in concrete under cyclic wetting and drying by electrical resistivity, *Cement and Concrete Composite*, Vol. 24, pp. 427-435.

Pont, S.D., and Ehrlacher, A., 2004. Numerical and experimental analysis of chemical dehydration, heat and mass transfer in a concrete hollow cylinder submitted to high temperatures, *Int. J. of Heat and Mass Transfer*, Vol. 47, pp. 135-147

Pruess, K., Oldenburg, C., and Moridis, G., 1999. *TOUGH2 User's Guide*, Version 2.0, Lawrence Berkeley National Laboratory, Berkeley.

Pruess, K., Simmons, A., Wu, Y.S., and Moridis, G., 1996. TOUGH2 Software Qualification Lawrence Berkeley National Laboratory, Berkeley, California.

Puyate, Y. T. and Lawrence, C. J., 1998, Chloride transport models for wick action in concrete at large Peclet number, *Physics of Fluids* , Vol. 10, No. 3.

Puyate, Y. T. and Lawrence, C. J., 1998. Wick action at moderate Peclet number, *Physics of Fluids* , Vol. 10, No. 8.
Richards, L.A. 1941. A pressure-membrane extraction apparatus for soil solution. *Soil Science*, Vol. 51, No. 5, pp. 377–386.

Ritcey, A.C., and Wu, Y.S. 1999. Evaluation of the effect of future climate change on the distribution and movement of moisture in the unsaturated zone at Yucca Mountain, NV. Journal of Containment Hydrology, vol. 38, pp. 257-279.

Rockhold, M. L., Fayer, M. J. and Heller, P.R., 1993. Physical and Hydraulic Properties of Sediments and Engineered Materials Associated with Grouted Double-Shell Tank Waste Disposal at Hanford. PNL-8813, Pacific Northwest laboratory, Richland, Washington

Romero, E., Gens, A., and Lloret, A. 2001. Temperature effects on the hydraulic behaviour of an unsaturated clay. *Geotechnical and Geological Engineering*, 19, pp. 311–332.

Scheidegger, A.E., 1974, The Physics of Flow Through Porous Media, *University of Toronto Press*, Toronto.

Saetta, A.V., Scotta, R.V. and Vitaliani, R.V., 1993, Analysis of Chloride Diffusion into Partially Saturated Concrete, *ACI Materials Journal*, 90-M47.

Savage, B.M. and Janssen, D.J., 1997, Soil Physics Principles Validated for Use in Predicting Unsaturated Moisture Movement in Portland Cement Concrete, *ACI Materials Journal*, 94-M8.

Samson, E., Marchand, J., Snyder, K.A., and Beaudoin, J.J., 2005, Modeling ion and fluid transport in unsaturated cement systems in isothermal conditions, *Cement and Concrete Research*, Vol. 35, pp.141-153.

Singh, D.N., and Gupta, A.K., 2000, Modelling hydraulic conductivity in a small centrifuge, *Canadian Geotechnical Journal*, **37**, 1150-1155.

Singh, D.N., and Kuriyan, S.J., 2002, Estimation of hydraulic conductivity of unsaturated soils using a geotechnical centrifuge, *Canadian Geotechnical Journal*, 39, 684-694.

Shi, C., 2004, Effect of mixing proportions of concrete on its electrical conductivity and the rapid chloride permeability test results, *Cement and Concrete Research*, 34, 537-545.

Standard Method of Test for Resistance of Concrete to chloride ion Penetration, 1980, T259-80, *American Association of State Highway and Transportation Officials*, Washington, D.C., U.S.A.

Stanish, K.D., Hooton, R.D., and Thomas, M.D.A., 1997, Testing the Chloride Penetration Resistance: a Literature Review, *FHWA Contract* DTFH61-97-R-00022.

Sosoro, M., and Reinhardt, H.W., 1996, The Modelling of Microstructure and Its Potential for Studying Transport Properties and Durability, Jennings, H., et al. (eds), *Kluwer Academic Publishers*, Netherlands, 443.

Tang, L., and Nilsson, L. O., 1992. Rapid Determination of the Chloride Diffusivity in Concrete by Applying an Electric Field, ACI Materials Journal, 89(1), pp. 49-53.

Tang, A., and Cui, Y., 2005. Controlling suction by the vapour equilibrium technique at different temperatures and its application in determining the water retention properties of MX80 clay. *Can. Geotech. J.*, Vol. 42, pp. 287-296.

van Genuchten, M.T., 1978, Calculating the Unsaturated Hydraulic Conductivity with a New Closed Form Analytic Model. Report 78-WR-08, *Princeton University*, Princeton, NJ

van Genuchten, M.Th., 1980. A closed-form equation for predicting the hydraulic conductivity of unsaturated soils. *Soil Sci Soc. Am J*,. 44:892-898**.**

van Genuchten, M.Th., Leij, F.J., and Yates, S.R., 1991, The RETC Code for Quantifying the Hydraulic Functions of Unsaturated Soils, *U.S. Salinity Laboratory, U.S. Department of Agriculture, Agricultural Research Service*, Riverside, California.

Khaleel, R., J.F. Relyea, and J.L. Conca. 1995. Evaluation of van Genuchten-Mualem relationships to estimate unsaturated hydraulic conductivity at low water contents. *Wat. Resour. Res*., 31(11):2659-2668.

Webb, S.W., and Phelan, J.M. 2003. Implementation of land surface boundary conditions in TOUGH2. TOUGH Symposium 2003 Proceedings.

Weyers, R. E. and Cady, P.D. 1987. Deterioration of Concrete Bridge Decks from Corrosion of Reinforcing Steel. *Concrete International*, American Concrete Institute, v. 9, No. 1, pp. 15-20.

Wexler, A. and Hasegawa, S. "Relative humidity-temperature relationship of some saturated salt solutions in the temperature range 0° to 50°C". J. Research NBS 53, 19 (1954)

Whitaker, S., 1977, Simultaneous heat, mass and momentum transfer in porous media: a theory of drying porous media, *Adv. Heat Transfer*, 119–203;

Whittington, H.W., McCarter, J., and Forde, M.C., 1981, The conduction of electricity through concrete, *Magazine of Concrete Research*, Vol. 33, No. 114, pp. 48-60.

Whiting, D., and Cady, P.D., 1992, SHRP-S/FR-92-109, *Strategic Highway Research program*, National Research Council, Washington, DC.